

Contract No:

This document was prepared in conjunction with work accomplished under Contract No. 89303321CEM000080 with the U.S. Department of Energy (DOE) Office of Environmental Management (EM).

Disclaimer:

This work was prepared under an agreement with and funded by the U.S. Government. Neither the U.S. Government or its employees, nor any of its contractors, subcontractors or their employees, makes any express or implied:

- 1) warranty or assumes any legal liability for the accuracy, completeness, or for the use or results of such use of any information, product, or process disclosed; or
- 2) representation that such use or results of such use would not infringe privately owned rights; or
- 3) endorsement or recommendation of any specifically identified commercial product, process, or service.

Any views and opinions of authors expressed in this work do not necessarily state or reflect those of the United States Government, or its contractors, or subcontractors.



**Savannah River
National Laboratory®**

A U.S. DEPARTMENT OF ENERGY NATIONAL LAB • SAVANNAH RIVER SITE • AIKEN, SC • USA

Characterization of the Insoluble Solids of the 241-17F and 241-49H Pump house Water Samples

F. F. Fondeur

September 2022

SRNL-STI-2022-00429, Revision 0

SRNL.DOE.GOV

DISCLAIMER

This work was prepared under an agreement with and funded by the U.S. Government. Neither the U.S. Government or its employees, nor any of its contractors, subcontractors or their employees, makes any express or implied:

1. warranty or assumes any legal liability for the accuracy, completeness, or for the use or results of such use of any information, product, or process disclosed; or
2. representation that such use or results of such use would not infringe privately owned rights; or
3. endorsement or recommendation of any specifically identified commercial product, process, or service.

Any views and opinions of authors expressed in this work do not necessarily state or reflect those of the United States Government, or its contractors, or subcontractors.

Printed in the United States of America

**Prepared for
U.S. Department of Energy**

Keywords: *Chromate water, Cooling water, insoluble solids*

Retention: *Permanent*

Characterization of the Insoluble Solids of the 241-17F and 241-49H Pump house Water Samples

F. F. Fondeur

September 2022

Savannah River National Laboratory is operated by Battelle Savannah River Alliance for the U.S. Department of Energy under Contract No. 89303321CEM000080.



REVIEWS AND APPROVALS

AUTHORS:

F. F. Fondeur, Separations Sciences and Engineering	Date
---	------

TECHNICAL REVIEW:

C. A. Nash, Separations Sciences and Engineering, Reviewed per E7 2.60	Date
--	------

APPROVALS:

M. Reigel., Manager, Separations Sciences and Engineering	Date
---	------

F. M. Pennebaker, Director, Chemical Processing and Characterization	Date
--	------

J. E. Burgin, Tank Farm Systems Engineering	Date
---	------

LIST OF REVISIONS

Revision Number	Summary of Changes	Date
0	Initial Issue	September 2022

ACKNOWLEDGEMENTS

The authors extend thanks to Analytical Characterization & Sample Management and Material Evaluation and NDE programs who assembled the test equipment, ran the experiments, and provided analytical results, specifically Henry Ajo, Catherine Housley, and Shirley McCollum.

EXECUTIVE SUMMARY

Six different water samples from 241-17F and 241-49H pump house were analyzed for chemical and physical characteristics as part of efforts to understand recent mechanical seal failures associated with four new cooling water pumps. A focus of this work was characterization of any “as found” insoluble solids. The insoluble material found in the FCRW (F-Area caustic water treated with sodium chromate at 241-17F) sample are mostly magnetite (Fe_3O_4 or possibly equipment rust) and silica. It was found that 26% of measured FCRW particles have at least one dimension larger than 15 microns. The insoluble particles found in the source water, domestic water (FDW), are mostly kaolin (aluminosilicate) and some iron oxide. All found FDW particles were larger than 15 microns. The insoluble particles of the other source water, F-Area well water (FWW), were mostly iron oxide with some trapped cations like calcium. Only 8% of found FWW particles were bigger than 15 microns.

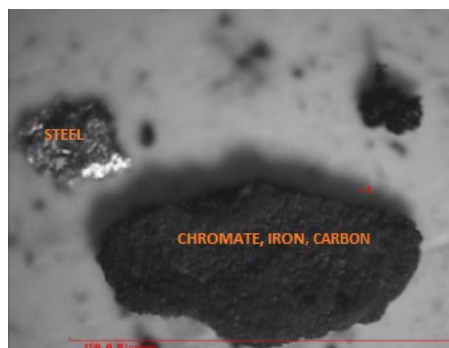
The insoluble particles found in the H-area chromate water (HCRW; caustic water treated with sodium chromate at 241-49H) are mostly iron oxide, chromate, and silica. Approximately 35% of HCRW particles were larger than 15 microns and had irregular shapes. The settled particles found in the domestic source water (HDW) were mostly silicates and iron oxide. At least 42% of HDW particles had one dimension larger than 15 microns. The other source of water in H-area, well water (HWW), had a noticeable amount of kaolin and gibbsite insoluble particles. Nearly 23% of HWW particles had at least one dimension larger than 15 microns.

A summary of the findings is listed below.

Analysis	FCRW	FDW	FWW	HCRW	HDW	HWW
Total volume (mL)	893	1082	1099	993	1078	1026
Liquid Density (g/mL at 22.7 °C)	0.9985	0.994	0.996	0.9984	0.9940	0.995
Insoluble solids (mg/L)	1.7	< 1.0	9.4	5.9	2.3	< 1.0
Soluble solids (mg/L)	1265*	84	28	1320*	28	102
Minerals	Magnetite, silica, quartz, copper, & chromium oxide	Kaolin & iron oxide	Lepidocrocite & magnetite	Lepidocrocite, magnetite, goethite, & chromate	Aluminosilicate & iron oxide	Kaolin, iron oxide & gibbsite
Mean size (μm)	11.4	120	7.2	17	37.5	9.3
% Of particles larger than 15 μm	26	100	8	35	42	23

*A little bit more than the calculated 450 ppm Na_2CrO_4 per liter and the addition of NaOH possibly due to carbonate formation in the sample during drying and above the 400 ppm recommend limit for this seal (Ref.2).

Large particles may strike the pump seal with sufficient energy to damage it (fracture). Small particles may enter narrow conduits and act like abrasives scratching or deforming or interrupting movement of surfaces. The particles appeared to have form (speculation) either during the preparation of the chromate water or during service from possible oxidation and/or reduction reactions with the chemicals and materials encountered by the chromate water. Particle formation and growth may also be occurring as a result of thermal aging, during pumping operation as a potential heat source. This is most clearly seen in the HCRW sample where different stages of particle growth were detected ($\text{Fe}^{2+} \Rightarrow \text{FeOOH} \Rightarrow \text{Fe}_3\text{O}_4$). Evidence of solid chromate was observed by the Fourier Transform Infrared Spectroscopy (FTIR). It is recommended that a combination of filtration, if it is not being done currently, and iron reduction is needed. A potential source of the iron can come from severe metal corrosion as well from the source water (well and domestic water). The presence of zinc may have originated from corrosion of galvanized mild steel that galvanically contacted either copper or aluminum alloy or other noble (more cathodic) metal. This is because groundwater is an unlikely source of detectable zinc. The oxidation-reduction reaction included the coprecipitation of chromate solids according to the FTIR. These hard solids (iron and chromate based) are hard enough to damage the surfaces of the pump seals. The solution might be oxidizing enough for any carbon surface to become oxidized (carbonyls) and drop out into the solution. A significant portion of the solids have a dimension larger 15 microns, and they represent a danger to the pump seal like the picture below shows.



Chemical addition to poison a corrosion reaction could be explored further but it is simpler to avoid using materials incompatible with the aqueous chemistry and eliminate galvanic coupling between metals of very dissimilar corrosion potential. For example, avoid coupling galvanized mild steel with copper or aluminum alloys. Note that some pump seals contain alumina, carbon, and stainless steel. Their degradation can also be a source of aluminum, iron and chrome. But the most likely scenario is that elements from the source water (like iron and aluminum) and elements from a possible corrosion of galvanized mild steel components (iron and zinc) formed solids and coprecipitated with the added chromate (after the pH was raised to 9) impacted the pump seals. In the case of F-area chromate water, iron and aluminum were already present in the F-area well water and coprecipitated with the caustic addition. The addition of $\text{NaCrO}_4 \cdot 10\text{H}_2\text{O}$ probably started corrosion of a possible galvanized mild steel (or a possible galvanic coupling between galvanized steel and aluminum or copper metal) leaching zinc ($\text{Zn}(\text{OH})_2$) and more iron coprecipitated with the iron and zinc to form iron chromate solids. In the case of the H-area chromate water, aluminum was coming from the domestic water but the $\text{NaCrO}_4 \cdot 10\text{H}_2\text{O}$ addition and possible galvanic coupling led to the leaching and then precipitation (due to the caustic environment) of zinc, iron, chromate, and aluminum. The H-area chromate water sample had the most solids. These solids are hard enough to damage a pump seal both by impact and by scratching inside gaps. This work measured all the particles larger than 15 microns to guesstimate the extent of the particle impact damage. 15-micron size is not an official size demarcation but particles with sizes larger than 15 microns will impart high impact kinetic energy to surfaces leading to their breakdown. The H-area chromate water had the most solids and the highest number of particles bigger than 15 microns. Recommended: Maintain insoluble and soluble solids concentration of the cooling water to just a few mg/L at most.

TABLE OF CONTENTS

1.0 Introduction.....	1
2.0 Sample Description/Experimental Set Up	2
3.0 Results and Discussion	6
3.1.1 FCRW, FDW, and FWW Samples	7
3.1.2 Particle size analysis of the FCRW, FDW, and FWW	14
3.1.3 Summary of the FCRW, FDW, and FWW samples	15
3.1.4 Analysis of the HCRW, HDW, and HWW samples.....	15
3.1.5 Particle size distribution of the HCRW, HDW, and HWW	21
3.1.6 Summary information of the HCRW, HWW, HDW, FCRW, FDW, and FWW.....	23
4.0 Conclusions.....	24
Appendix A: SRNL Scope for the Characterization of the soluble and insoluble portions of the FCRW, FDW, FWW, HCRW, HDW, and HWW water samples.....	26
Appendix B. Examples of particle size distribution of different images from different sources (SEM, optical photography, and optical microscopy).	27
Appendix C. Analytical Methods.....	29
Appendix D. Personal communication with Eric Burgin	30

LIST OF TABLES

Table 1. ICP-OES of digested FCRW, FDW, FWW (ug/g _{slurry}), and solids from FCRW (mg)	13
Table 3. ICP-OES analysis of the slurry samples from HCRW, HDW, HWW slurries (ug/g _{slurry}) and solids from HCRW (mg).....	20
Table 4. Summary Information of the HCRW, HDW, HWW, FCRW, FDW, and FWW	23

LIST OF FIGURES

Figure 1 Pictures of the “as received” water samples: A) FCRW, B) HCRW, C) FWW, D) HDW, E) FWW, and F) FDW.....	4
Figure 2 Retentate weight from A) FCRW (1.5 mg/892 mL), B) HCRW (5.8 mg/992 mL), C) FDW (< 1 mg/1083 mL), D) HDW (2.6 mg/1078 mL), F) HWW (< 1mg/1026 mL), and F) FWW (11 mg/1099 mL).	5
Figure 3. XRD Spectra of the solid samples: A) FCRW (magnetite, SiO ₂ , quartz), B) FDW, and C) FWW (lepidocrocite and magnetite) solid particles	8
Figure 4. FTIR analysis of the FCRW, FDW, and FWW solids.	9
Figure 5. Representative EDS spectrum of the FCRW, FWW and FDW solid particles	10
Figure 6. Representative XRF elemental composition of the A) FCRW, B) FDW, and C) FWW	12
Figure 7. Particle size distribution of A) FCRW, B) FWW, and C) FDW. Note: Microtrac results are shown for the FWW sample. Histogram of photos are shown for the FCRW and FDW samples.	14
Figure 8. XRD spectra of the HCRW, HDW, and HWW solid samples.....	16
Figure 9. FTIR of the HCRW, HDW, and HWW solids.	17
Figure 10. SEM/EDS analysis of the A) HCRW, B) HDW, and C) HWW samples.....	18
Figure 11. XRF elemental composition of A) HCRW, B) HDW, and C) HWW.....	19
Figure 12. Particle size analysis of the HCRW, HDW, and HWW samples.	22
Figure 13. An example of a black and white image segmentation done with an SEM image of the HWW solids. Segmented image does not include captions of the original image (top)	27
Figure 14 An example of a black and white image segmentation done with an BE image of the FCRW solids. Segmented image does not include captions of the original image (top)	28
Figure 15. An example of image segmentation (images with red particles) of the optical microscope images of FDW solids.....	29

LIST OF ABBREVIATIONS

AQR	aqua regia digestion
FT-IR	Fourier transform infrared
ICP-OES	inductively coupled plasma optical atomic emission spectroscopy
BDL	below instrument detection limit
CSTF	Concentration Storage and Transfer Facility
FCRW	F-Area water from 241-17F containing 450 ppm sodium chromate
FDW	F-Area domestic water
FTIR	Fourier transformed infrared spectroscopy
FWW	F-Area well water
HCRW	H-Area water from 241-49H containing 450 ppm sodium chromate
HDW	H-Area domestic water
HWW	H-Area well water
M&TE	Measurement and Test Equipment
PF	Peroxide fusion
PSA	Particle size analysis
PDS	Particle size distribution
SEM/EDS	scanning electron microscope/energy dispersive x-ray spectrometry
SRNL	Savannah River National Laboratory
SWPF	Salt Waste Processing Facility
SRS	Savannah River Site
XRF	X-ray Fluorescence
XRD	X-ray diffraction

1.0 Introduction

The Savannah River Site (SRS) 241-17F and 241-49H pump house facilities are designed to pump chromate cooling water through radioactive liquid waste tanks in H and F tank farms. The mechanical seals for these pumps are cooled via pump mounted flush lines with chromate water (CRW). Chromate water is water from either a well water (WW) and/or domestic water (DW) source that is treated with 450 ppm sodium chromate (for corrosion control or metal passivation) and sodium hydroxide until the pH is greater than 8. Recently, these facility pumps have experienced frequent pump seal failures (leaks) that resulted in frequent operation interruptions (see figure below for a typical inexpensive pump seal). Personnel have outlined several scenarios for the pump seal failures. One scenario speculates that the presence of large particles in the CRW may lead to the erosion of the pump seals. To determine the validity of this theory, six water samples (HDW, HWW, HCRW, FDW, FWW, and FCRW) collected by scooping a known volume from mixed tanks were sent to SRNL for analysis.¹

The work scope for these water samples involves the physical (particle size) and elemental characterization (and compound identification as able) of the “as-received” water samples from the April 2022 241-17F and 241-49H pump house facilities. The water samples included F-area domestic water (FDW), F-area well water (FWW), F-area chromate water (FCRW), H-area domestic water (HDW), H-area well water (HWW), and F-area chromate water (FCRW). The well water and domestic water are the source water for the chromate treated water (CRW). Where required, these water samples were to be characterized using x-ray diffraction (XRD),¹ scanning electron microscope/energy dispersive x-ray spectrometry (SEM/EDS), X-rays fluorescence spectrometry (XRF), particle size analysis (PSA-Microtrac), Fourier transform-infrared (FT-IR) and inductively coupled plasma optical emission spectroscopy (ICP-OES) to characterize and identify inorganic components in the water samples as part of efforts to understand the problems occurring at 241-17F and 241-49H pump house facilities.

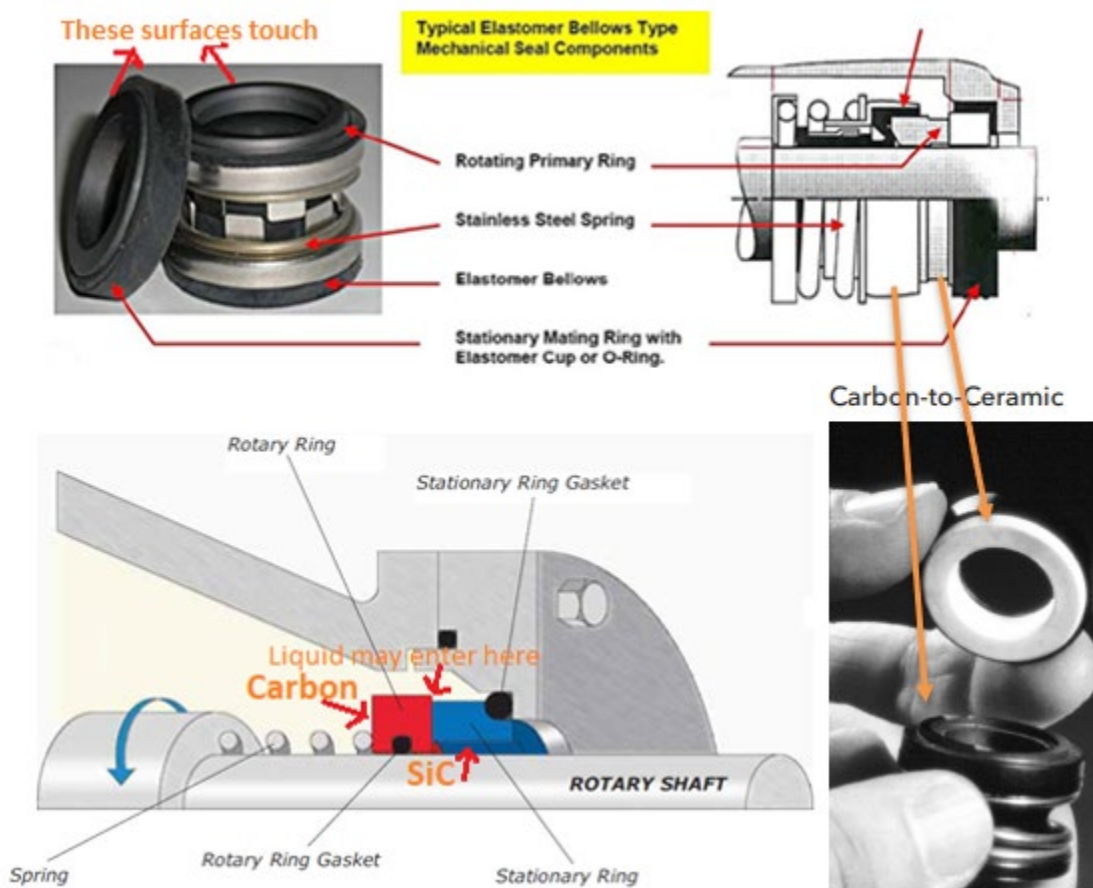
The Tank Farm customer requested the characterization¹ of the “as-received” 241-17F and 241-49H water samples (April 2022) as summarized in Appendix A. Chromate water is made slightly caustic by adding sodium hydroxide and to keep the chromate ion species from reacting (to prevent formation of Cr^{6+}). Sodium chromate is added to water as a corrosion inhibitor for closed cooling water systems. Chromate treatments in the range of 500 to 1,000 parts per million (ppm) are satisfactory for single metal surfaces. Improved effectiveness requires pH control in the range of 7.5 and 9.5. Limits on chromate inhibitor corrosion inhibitor concentrations are needed to protect carbon (the material of the original seals are carbon on the rotary face and silicon carbide in the stationary face) mechanical seals from large particles and in applications with a very high heat transfer rate (such as in pumps) although the carbon face prevents the face of the seal from burning up during a dry start-up. However, carbon is prone to surface oxidation (carbonyls) at high temperature that may change its surface mechanical properties. Carbon can be graphite or amorphous carbon or a compound of these two but is not which carbon is used at 241-17F and 241-49H. A high concentration of insoluble materials can be damaging to pump seals. One vendor stated that the Buna/C/SiC seal cannot handle any silica or 20 ppm insoluble solids or 400 ppm soluble solids or pH higher than 9.²

Pump seals prevent pumps from leaking, and they contain the pressure of the pumping process while resisting the friction caused by the pump shaft rotation. Pump seals are typically made of ceramic (stator) and carbon (rotor) (see figure below). The seals in question have a silicon carbide stator and a carbon rotor.

¹ Technical assistance request (TAR) M-TAR-G-0006

² RL Deppman, “How to pick an HVAC Centrifugal Pump Part 7: Mechanical Seal Materials. As of September 19, 2022, https://www.deppmann.com/wp-content/uploads/2017/07/RLD_MMM_Mechanical_Seal_Materials.pdf

The remaining parts are typically made of stainless steel and some elastomers. Assuming the pumps were not run dry or installed incorrectly or the pump's shaft had no wobble, or the temperature rise was not significant, and that cavitation did not play a role, the possible pump's seal damage scenario might be chemical attack and/or solids ingress. Pump seals are judged by their hardness, stiffness, chemical compatibility, and thermal conduction. Typically, pump seals (of this type of materials) are not tolerable of any insoluble solid concentration and high soluble solid concentration. This study focuses on the chemistry of the water and any possible solid that can cause damages (and change in tolerance) to the pump's seals.



2.0 Sample Description/Experimental Set Up

In April 2022, tank farm operations personnel collected the HDW, HWW, HCRW water sample and the FDW, FWW, and FCRW sample from the 241-49H and 241-17F facility, respectively. A picture of the "as received" water samples is shown in Figure 1. The HCRW and FCRW samples were slightly radioactive (< 30 dpm/mL beta gamma per Radcon survey) and therefore, they were received and processed in a radioactive chemical hood.

The density and temperature of the liquids were measured with an Anton Paar vibrating tube. The density of the air and of doubled-distilled and de-ionized water were measured before and after the liquid measurements. The recorded numbers were consistent with literature values.

For gravimetric measurements, M&TE certified balances with a 0.1 mg resolution and a 1 mg uncertainty were used (Mettler-Toledo). The balances were checked before their use with M&TE certified weights to verify their performance (accuracy, dispersion, and linearity). For drying the samples, they were placed in convective hot air ovens set at 105 Celsius (± 0.5 Celsius with M&TE type K thermocouples). The sample

weights were monitored and recorded daily until the sample weight change was less than uncertainty of the balance (< 1 mg). At that point, the samples were considered dried. Samples were then repackaged and submitted to SRNL Analytical Characterization and Management group for additional analysis.

The “as received” liquid samples were agitated (by vigorous end over end rotations and back and forward shaking motions for approximately 35 seconds) to ensure a well-mixed aliquot, an approximately 15 mL portion of the slurry (by volume) was removed and digested with Aqua Regia (50 mL dissolution or 3.26 mL/g) and analyzed for ICP-OES. The rest of the samples were filtered with a 0.45 microns polyether sulfone filter (as received filter paper weights were recorded). The loaded filters were then rinse with 15 mL of water and then dried in an oven at 45 Celsius (the filter papers were covered to prevent solid deposition from the oven). The weights of the filters were recorded as well as that of “as received” filter with no retentate. Portions of the retentate (solids on filter) were sent for XRD, XRF, SEM-EDS, and Fourier-Transform Infrared (FTIR). The remaining retentates were digested with peroxide fusion and submitted for ICP-OES analysis.

Optical pictures of the “as received” samples are shown in Figure 1. The pictures show the relative amounts of solids at the bottom of the samples.

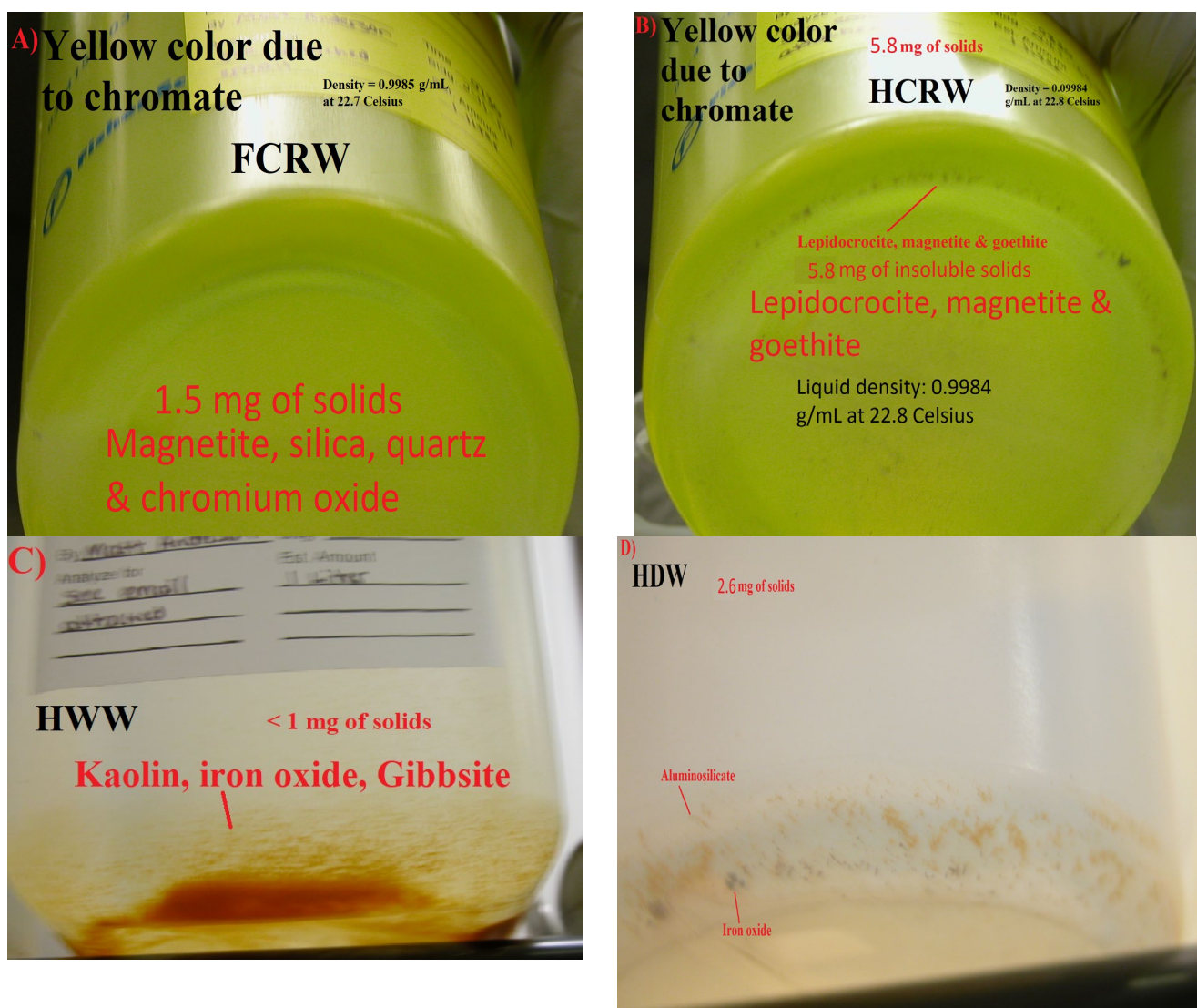




Figure 1 Pictures of the “as received” water samples: A) FCRW, B) HCRW, C) FWW, D) HDW, E) FWW, and F) FDW.

Separation of the suspended and settled solids in the water samples was attained by filtering the samples through a 0.45 microns polyether sulfone filter paper (water rinsed and then oven dried). The filter papers with the solids are shown in Figure 2. Approximately 1.2 mg of dried solids were recovered from the FCRW liquid sample that appeared to contain no settled solids upon visual inspection of Figure 1A, but a noticeable solid layer was retained in Figure 2A. On the other hand, a visually colored layer (brown color) of solids was observed in Figure 2F but its corresponding weight was within the uncertainty of the balance (~ 1mg), indicating very little retained solids. The highest amount of retained solids was obtained with the FWW sample (Figure 2F). Soluble solids were determined by drying 50 mL of the filtered supernate (placed in glass beakers) in an oven at 110 Celsius.

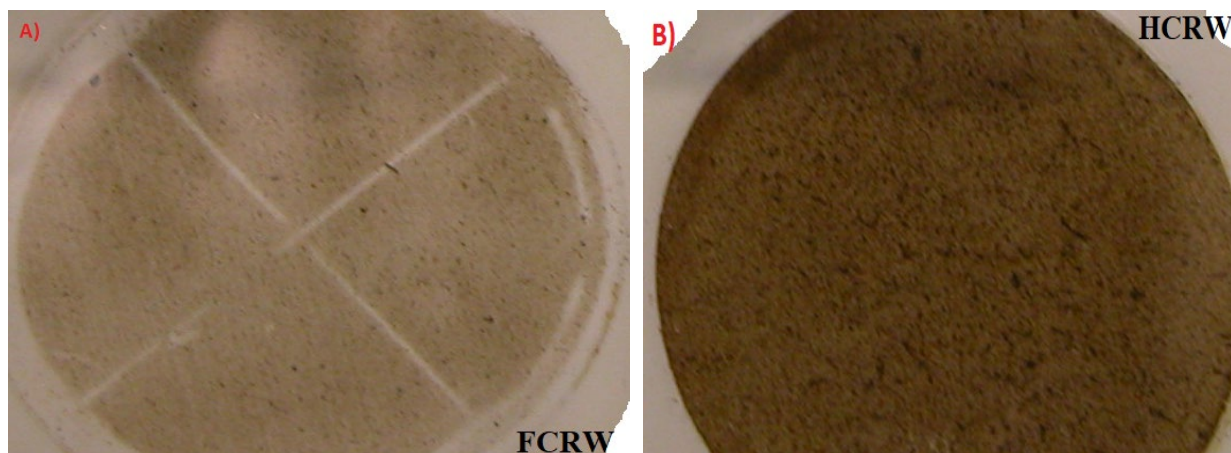




Figure 2 Retentate weight from A) FCRW (1.5 mg/892 mL), B) HCRW (5.8 mg/992 mL), C) FDW (< 1 mg/1083 mL), D) HDW (2.6 mg/1078 mL), E) HWW (< 1mg/1026 mL), and F) FWW (11 mg/1099 mL).

Personnel cut pieces of the filters (approximately $\frac{1}{4}$ of slice from the original filter or 8.52 cm²) and submitted them for XRD, XRF, SEM/EDS, and FTIR analysis.

Identification of crystalline compounds whenever possible was obtained with a XRD instrument from Rigaku. The Rigaku Smart Lab is a theta-theta diffractometer that can accommodate a variety of optical components. It consists of an x-ray source (3kW Cu tube) and two detectors – a 0D scintillation detector and a 0D, 1D, 2D HyPix detector. In addition, the instrument has an in-plane detector arm, Phi (sample rotation), and Z (sample height).

FTIR analysis of the samples was done with a Nicolet Nexus 670 equipped with a Continuum™ microscope.

Large area elemental composition of the samples was obtained by the XRF method with Mini-X2 X-ray tube from Amptek. The probe was operated with a maximum high voltage of 50 kV and a maximum power

of 10 W. Anode material included Ag, Au, and W. XRF has low sensitivity for lighter elements below aluminum ($Z < 13$).

Small area elemental composition was obtained with a LEO S440 SEM/EDS spectrometer. The LEO S440 contained scanning electron microscope (CSEM), with an accelerating voltage up to 30 kV and capability of secondary electron imaging, backscatter electron imaging, and X-ray microanalysis, is contained in a radiological glovebox train with hood that has sample preparation equipment such as carbon and gold coating and a stereomicroscope with image capture. The radiological glovebox enclosure of sample preparation instrumentation and CSEM allows sample preparation and analysis of radioactive materials. This instrument includes an Oxford Instruments energy dispersive spectrometer (EDS) for detection of elements greater than atomic number 3 ($Z > 3$ or beryllium) and an Oxford Instruments wavelength dispersive X-ray spectrometer (WDS) for lower detection limits, resolution of EDS overlaps, and higher resolution X-ray collection. The Oxford Instruments INCA 4.15 software package allows for standardless semi-quantitative analysis, elemental mapping, and simultaneous EDS/WDS measurements. Magnification is checked using NIST SRM-1961 polystyrene spheres. EDS is checked by measuring the copper EDS spectrum using copper tape.

If samples charge under the electron beam, they are coated with carbon or gold until the charging drops to acceptable levels as seen in SEM imaging.

Particle size measurements were obtained using a laser light scattering method with a Microtrac 3500 equipped with an optical bench and a wet sample delivery controller (SDC). The SDC flow rate was set to 30% for background measurements and analysis measurements. The analysis conditions for the instrument were set to account for irregular particle shapes, particles that absorb the laser light, and to measure the particles for 30 seconds three times and report an average of those. A large slurry pipette with the bulb depressed was placed in the bottle and as the bulb was released the pipette was pulled up in the bottle. The liquid in the pipette was added to the SDC until the Microtrac software indicated enough sample had been loaded to perform the analysis several sample draws were made from the bottle to achieve this. At the conclusion of the analysis, Microtrac's proprietary mathematical software generated a report containing the tabular data, a histogram plot of the data, and the instrument parameters.

In some cases, the samples had solid concentrations below the Microtrac 3500 concentration limit. In those cases, the optical microscopy pictures were collected and analyzed with an imaging software ImageJ³ from the National Institute of Health. The analysis provided particle size distribution as well as parameters related to the particles irregular shape.

3.0 Results and Discussion

The density of the liquid portion of the FDW, FWW, HDW, and HWW samples were very close to that of water (0.9974 at 22.7 °C). The density of the liquid portion of the FCRW and HCRW samples were 0.9984 and 0.9985 g/mL at 22.7 °C respectively. The pH value of these samples was nine (pH paper). No viscosity or surface tension measurements were performed.

³ ImageJ is an imaging software open to the public at <https://imagej.nih.gov/ij/>

3.1.1 FCRW, FDW, and FWW Samples Chemistry (elemental and compound)

The XRD spectra of the FCRW, FWW, and FDW solid samples are presented in Figure 3. The XRD spectra for all three samples, as shown in Figure 3, indicate the presence of a large background shift due to the presence of amorphous due to the filter paper (PES) that supports the solids. The XRD spectrum of the FCRW has matching peaks for crystalline inorganic minerals like magnetite [Fe_3O_4], silicon dioxide (SiO_2), and Quartz (SiO_2). $\text{Fe}(\text{OH})_x^{3-x} \Rightarrow \text{Fe}_3\text{O}_4$ when the pH is above 8 and some heating is involved.⁴ The XRD spectrum of the FWW samples has matching peaks with minerals like lepidocrocite (FeOOH ; an oxyhydroxide of iron or stable phase between iron hydroxide and iron oxide) and magnetite. This spectrum was collected for 6 hours. The XRD spectrum of the FDW sample was featureless (Figure 3B).

The FTIR spectra of the FCRW, FWW, and FDW solid samples are shown in Figure 4. The closest identified compounds in the FCRW samples were silicates and hydrous chromium oxide (CrO_4^{2-}). Somehow, chromium is being coprecipitating. Chromate anions (CrO_4^{2-}) can react with metals (or oxides) of aluminum, zinc, and iron to form chromium chromate solids (these solids may have both Cr^{3+} and Cr^{6+}). These solids tend to be abrasive. It is difficult to ascertain if the chromate observed here may have come from the deterioration of chromate anodized aluminum parts. Lepidocrocite (FeOOH), silica, nitrates and carbonate were identified in the FTIR spectrum of the FWW solids. The FTIR spectrum of the FDW solids indicated the presence of kaolin and carboxylate groups. No chromium oxide was observed in the FDW and FWW solids as expected.

The principal SEM/EDS elemental compositions for the FCRW, FWW, and FDW samples are shown in Figures 5. The principal components in the FCRW samples are iron (Fe), silicon (Si), chromium (Cr), zinc (Zn), and aluminum (Al). Iron was seen in all three samples as expected since it is naturally found in the soil. However, iron from a corrosion process is also possible. Chromium is consistent with the chromium oxide observed by the FTIR (Figure 4), but it is added to a level that avoids its precipitation. Elements found in the FWW sample included iron, silicon, and aluminum. The observed Si and Al are consistent with the SiO_2 found in the FTIR of this sample. Lots of iron debris was found in the FWW sample (cold working or impact damage). The FDW sample contains Al, Si, Fe, Ca (calcium), chloride (Cl), potassium (K), and magnesium (Mg). These elements (Si and Al) are consistent with the kaolin detected by the FTIR.

An independent way of confirming the elemental composition of the samples is XRF. Figure 6 shows the XRF spectra of the three samples. The major elements in the FCRW sample (Fe, Zn, Ca, K, and copper (Cu)) as found by the XRF are consistent with the elements found in the EDS spectrum. It is a bit surprising that no Si and/or Al were observed. The XRF spectrum of FDW sample showed Fe, nickel (Ni), Cu, Cr, K, yttrium (Y), chloride (Cl), and Ca. These elements are consistent with the findings of the EDS analysis. Yttrium is commonly found in the soil. The FWW sample contain Fe, Zn, Cu, Ni, Cr, Ca, Al, Cl, and manganese (Mn). Some of these elements are consistent with the EDS analysis. Nickel is rarely found in natural groundwater, but it is common in corrosion of water delivery systems. No Si was observed which is not consistent with the observation of silicon dioxide.

⁴ C. J. Dodge, A. J. Francis, J. B. Gillow, G. P. Halada, C. Eng, & C. R. Clayton, "Association of uranium with iron oxides typically formed on corroding steel surfaces", *Environ. Sci. Technol.* 2022, 36 3504-3511.

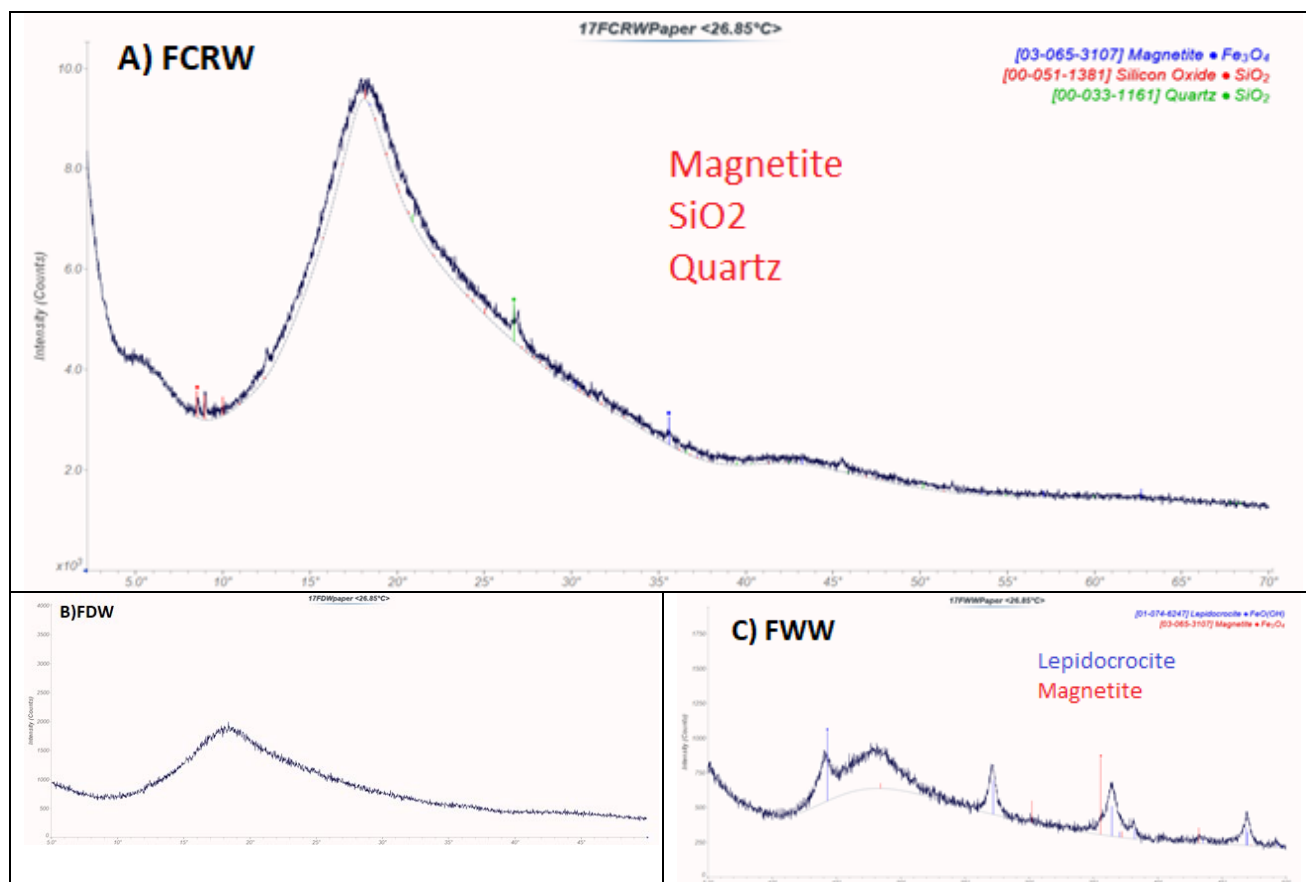
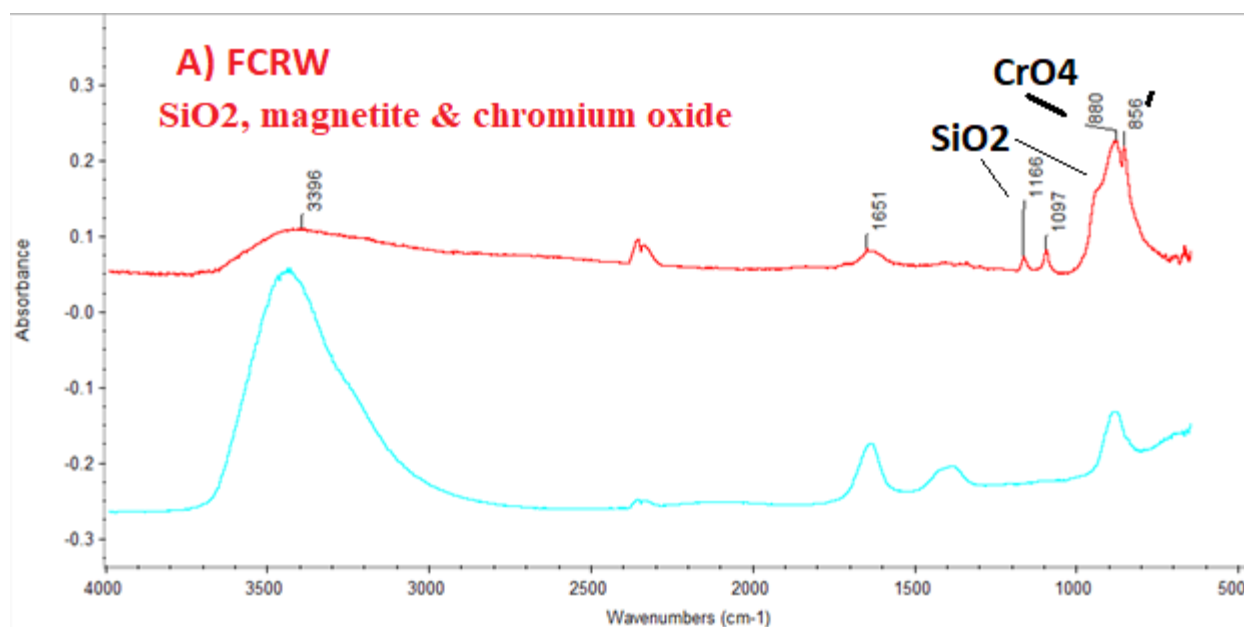


Figure 3. XRD Spectra of the solid samples: A) FCRW (magnetite, SiO_2 , quartz), B) FDW, and C) FWW (lepidocrocite and magnetite) solid particles



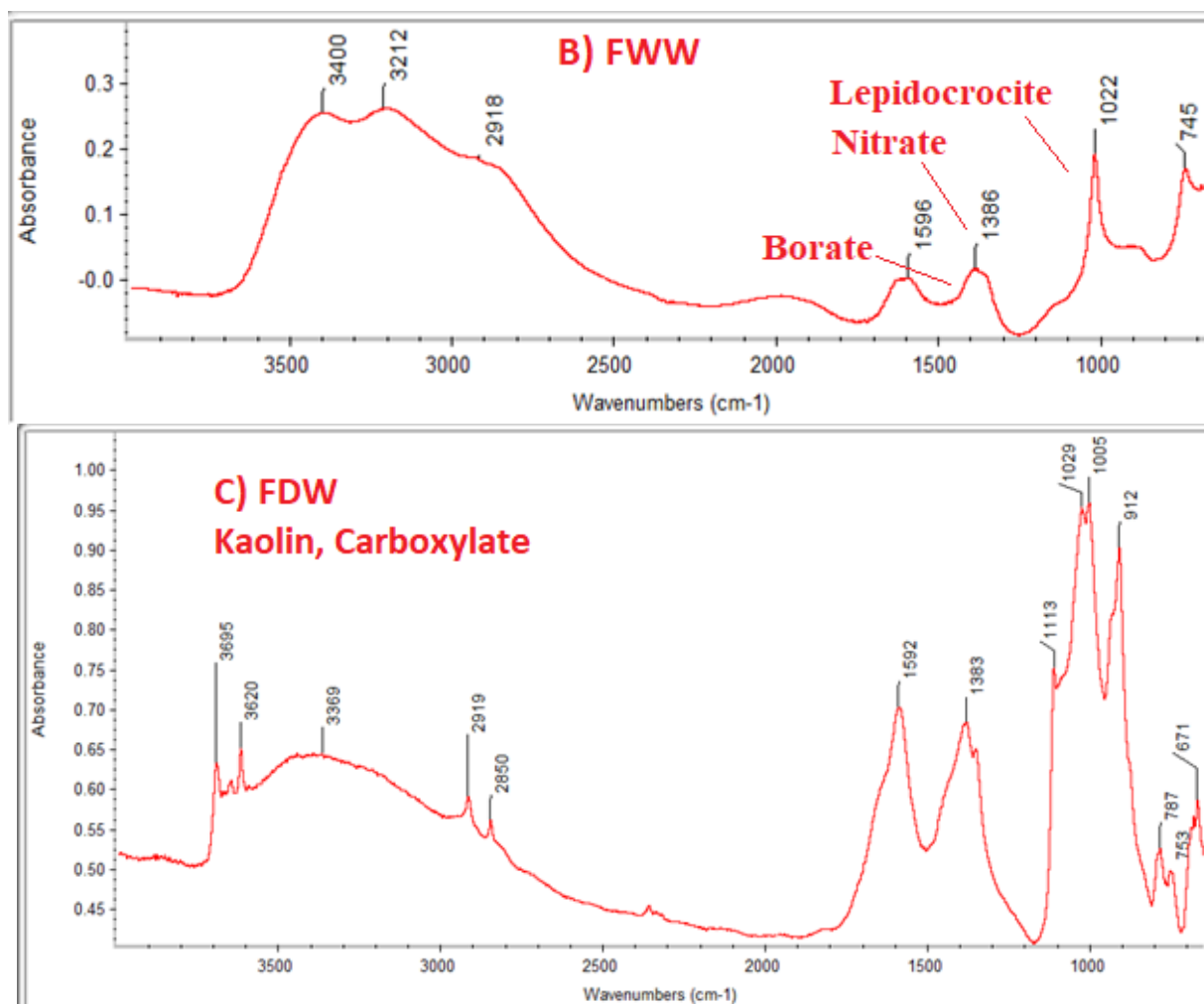
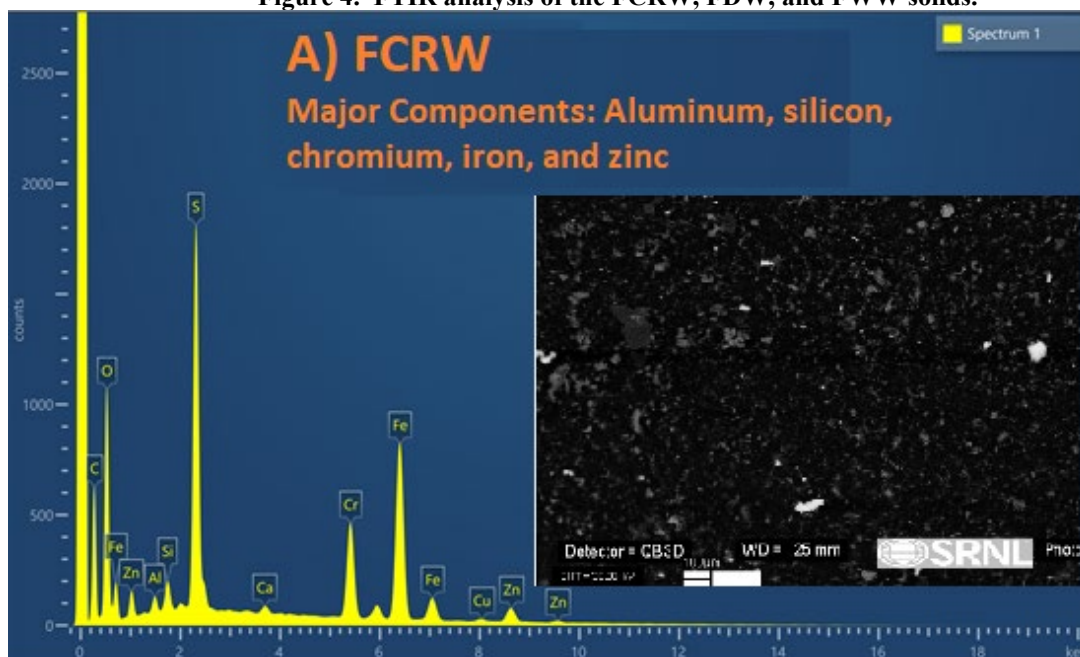


Figure 4. FTIR analysis of the FCRW, FDW, and FWW solids.



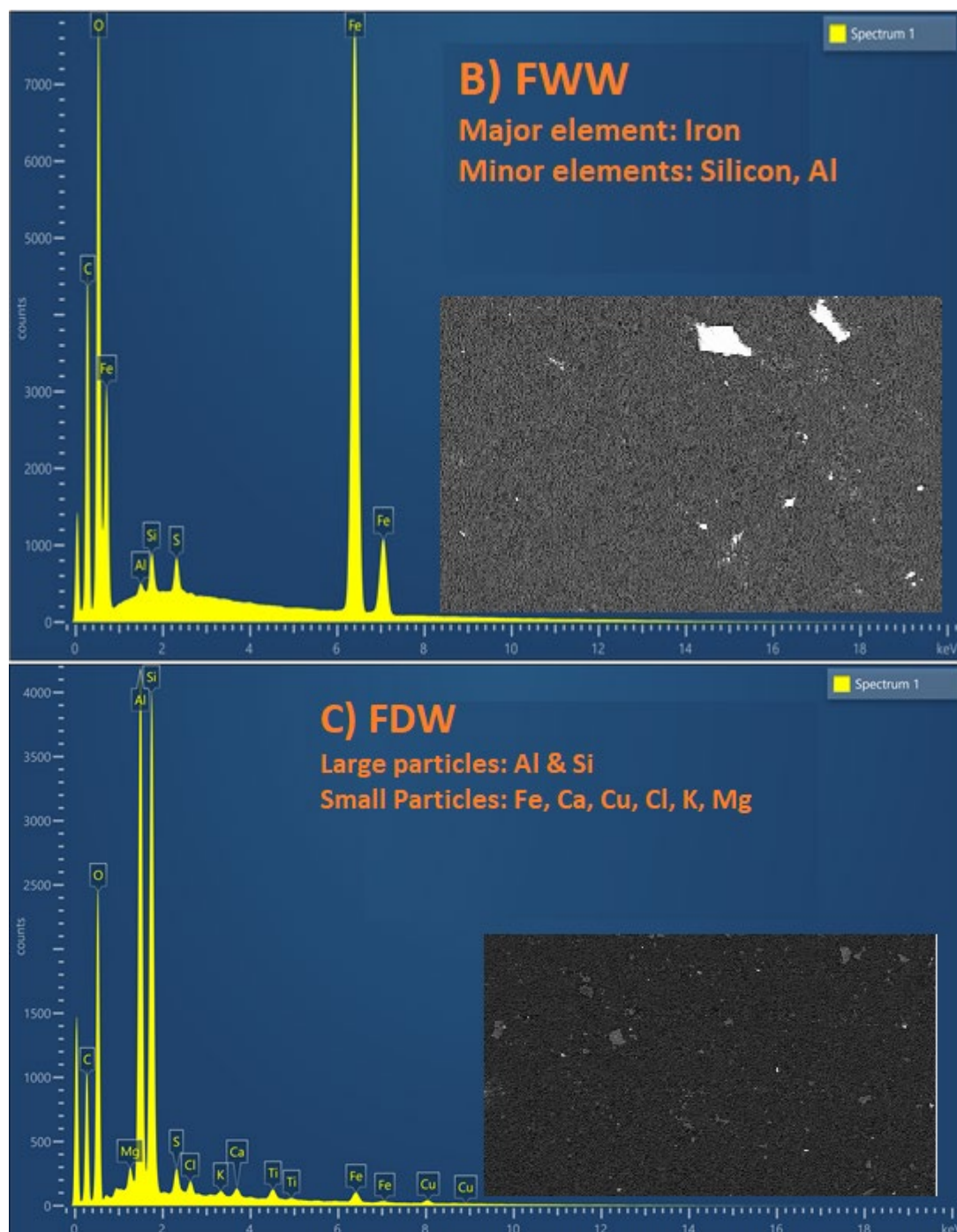
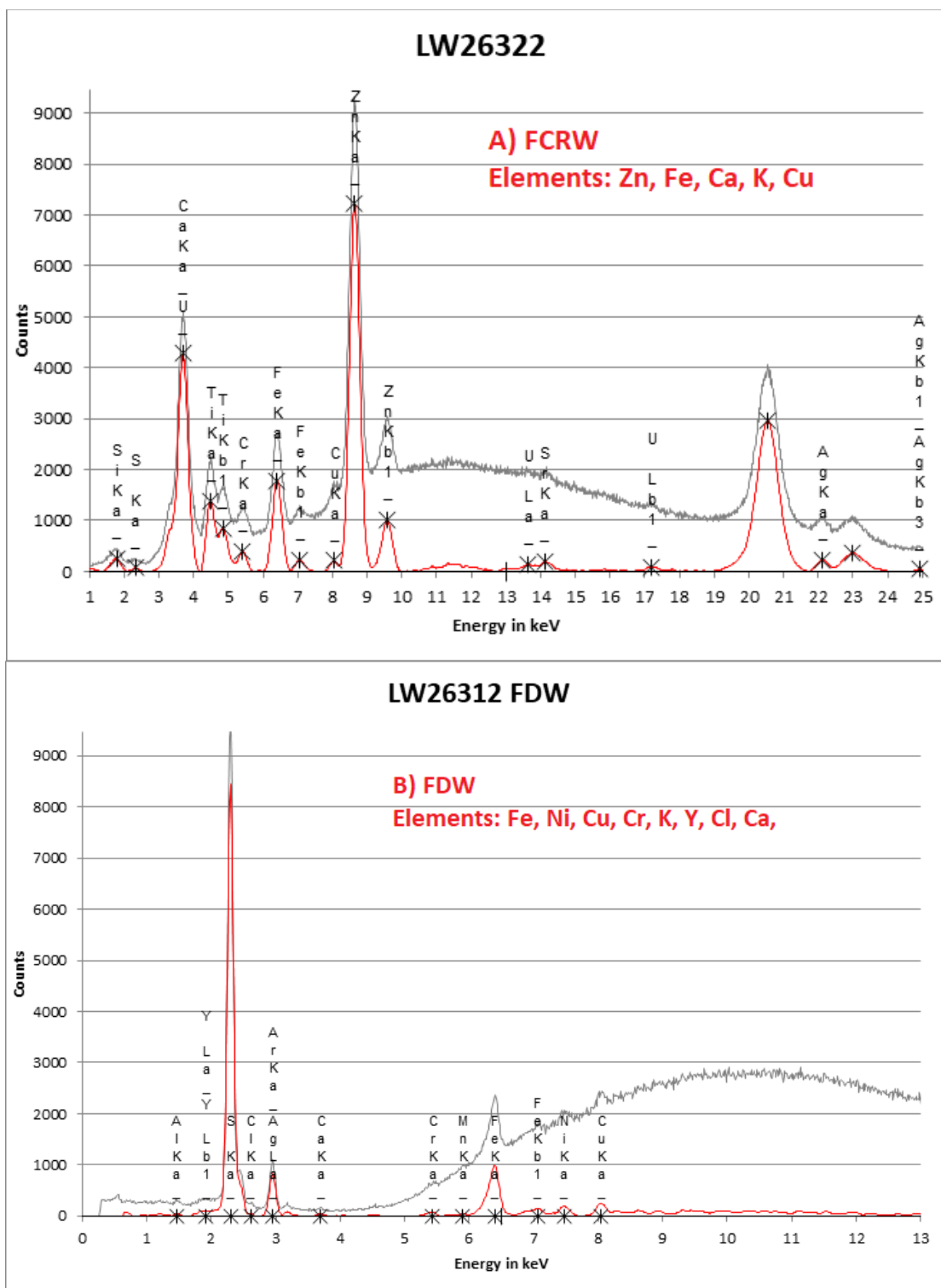


Figure 5. Representative EDS spectrum of the FCRW, FWW and FDW solid particles



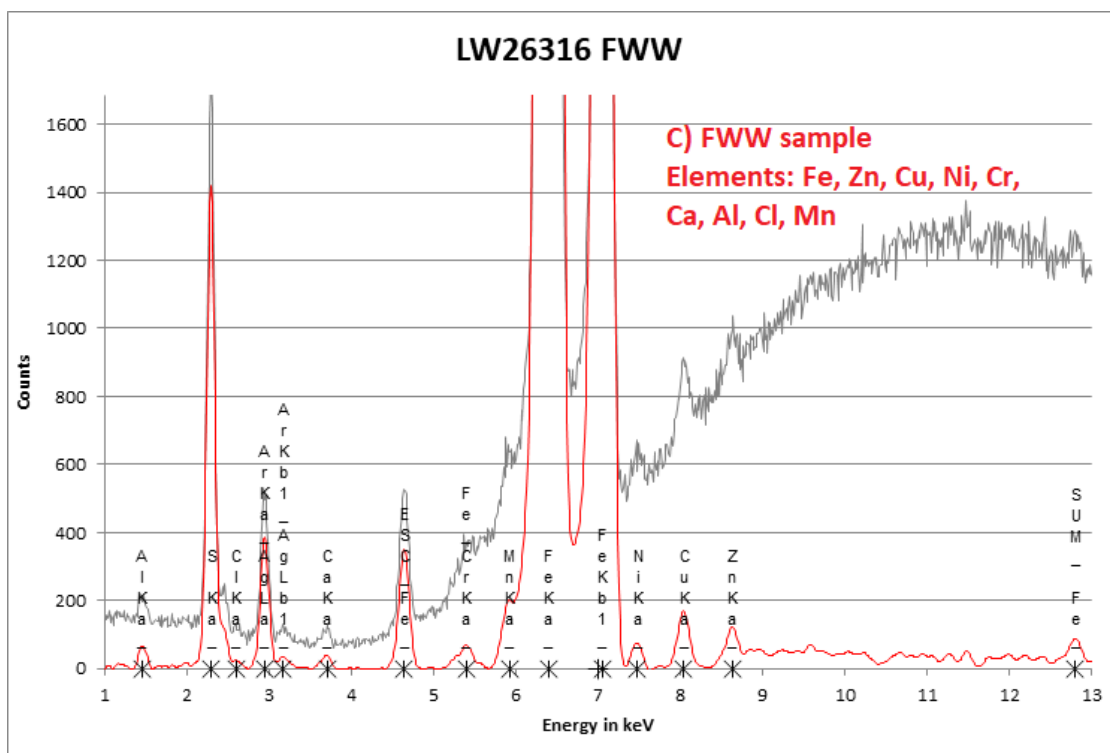


Figure 6. Representative XRF elemental composition of the A) FCRW, B) FDW, and C) FWW

The slurry samples were digested by Aqua Regia (AR) and the digested sample analyzed by ICP-OES. Table 1 lists the elemental composition. Sample FCRW contains boron (B), barium (Ba), Ca, Cr, Fe, Mg, sodium (Na), sulfur (S), Si, and Zn. Aluminum was not observed in the FCRW slurry, but it was detected in the EDS and implicitly detected in the FTIR analyses. Boron was not observed in any of the elemental analysis of the solid samples. All three samples (FCRW, FWW, and FDW) have similar elemental composition with the exception that both Cr and Zn are found in the FCRW sample. Cr is purposely added to this source water (not likely from the oxidation of chromium metal in caustic solution), and it is speculated that Zn may be a contaminant but likely from corrosion of galvanized low carbon steel. The lower concentrations of Ca, Fe, Si, and B values in the FCRW suggest they precipitated out. This is consistent with the iron oxide and silica found by XRD and FTIR. Table 1 also shows the chemical analysis of the digested solids from the FCRW sample. The analysis indicates that Al, Fe, Cr, and Zn were the major elements detected. These elements were the same seen in the HCRW samples. They appear to indicate that a precipitation reaction occurred possibly from increasing the pH to 9 in these samples. It is likely the zinc, which is not abundant in groundwater, indicates that galvanized mild steel may have come in contact (galvanic coupling) with another metal (like copper or aluminum) to cause its dissolution. The iron may have come from both the water sources and mild steel corrosion. Chromium possibly from the chromate addition to the water and it participated in the corrosion reactions (for example, oxidizing iron to iron oxide). Chromium is also a component of stainless steel, but it is unlikely that stainless steel corrosion occurred in these conditions. The chromium is most definitely coming from the chromate addition and possibly from the pump seal degradation (most pump seals contain both silicon carbide and stainless steel). As determined by the FTIR data, chromate appeared to have coprecipitated (chromate peak at 880 cm^{-1}) possibly from pH changes or redox reactions. Recall that there is chromate in solution but chromate from stainless steel corrosion is also possible but less likely.

Table 1. ICP-OES of digested FCRW, FDW, FWW (ug/g_{slurry}), and solids from FCRW (mg)

Element	FDW	FWW	FCRW	FCRW solids (mg) #
Ag	< 0.178	< 0.17	< 0.168	< 0.054
Al	< 0.103	0.152	< 0.097	0.088
B	0.850	0.800	0.357	< 0.0034
Ba	0.148	0.142	0.117	< 0.009
Be	< 0.0017	< 0	< 0.0016	< 0.001
Ca	1.59	2.93	0.325	0.406
Cd	< 0.0022	< 0	< 0.0021	< 0.0012
Ce	< 0.0689	< 0.07	< 0.0648	< 0.0745
Co	< 0.022	< 0.02	< 0.021	< 0.0015
Cr	< 0.037	< 0.04	314	0.039
Cu	< 0.065	< 0.06	< 0.061	< 0.0172
Fe	0.197	7.89	0.486	0.094
Gd	< 0.095	< 0.09	< 0.089	< 0.0018
K	< 0.842	< 0.82	< 0.793	< 0.198
La	< 0.0045	< 0	< 0.0042	< 0.0014
Li	< 0.0606	< 0.06	< 0.0571	< 0.018
Mg	0.280	0.422	0.056	0.048
Mn	< 0.017	0.143	< 0.016	< 0.006
Mo	< 0.028	< 0.03	< 0.027	< 0.004
Na	29.9	4.45	356	NR
Ni	< 0.023	< 0.02	< 0.021	< 0.002
P	0.352	< 0.07	< 0.064	< 0.016
Pb	< 0.0612	< 0.10	< 0.0577	< 0.019
S	0.556	0.637	3.23	1.735
Sb	< 0.0413	< 00	< 0.0389	< 0.01
Si	4.74	1.50	1.72	< 0.121
Sn	< 0.204	< 0.2	< 0.192	< 0.062
Sr	< 0.012	< 0.01	< 0.012	< 0.002
Th	< 0.102	< 0.1	< 0.0957	< 0.01
Ti	< 0.0405	< 0.04	< 0.0382	< 0.007
U	< 0.246	< 0.24	< 0.232	< 0.026
V	< 0.032	< 0.03	< 0.030	< 0.01
Zn	< 0.048	< 0.05	0.267	0.0394
Zr	< 0.0055	< 0.01	< 0.0051	NR

NR stands for "not reported". # Digested solids

Comparing the elemental and FTIR analysis of the solid particles, the FCRW solids appear to have formed in the chromate water rather than direct solids transfer from either the domestic water or well water. It is possible that an oxidation and/or reduction reaction occurred that precipitated chromium, aluminosilicate (aluminum and silicon possibly from the F-Area well water and driven by temperature

and solubility) and Iron oxyhydroxide and oxide. The iron could have been a direct transfer from the source water, but it can also be a corrosion product occurring at the pumps.

3.1.2 Particle size analysis of the FCRW, FDW, and FWW

Two approaches were used for determining the particle size distribution (PSD) depending on the concentration of solids in the samples. Microtrac analysis was possible only with the FWW sample (concentration above 0.01% v/v). Image analysis of optical images was used to determine PSD of samples with a low solid concentration. Recall, results from laser scattering (Microtrac) may differ from the results of analyzing an optical picture of particles on a filter paper especially if the particles have irregular shapes.

Figure 7 shows the PSD results from the Microtrac of the FWW sample (Figure 7B), and the PSD derived from analyzing the optical microscope pictures of FCRW (Figure 7A) and FDW (Figure 7C).

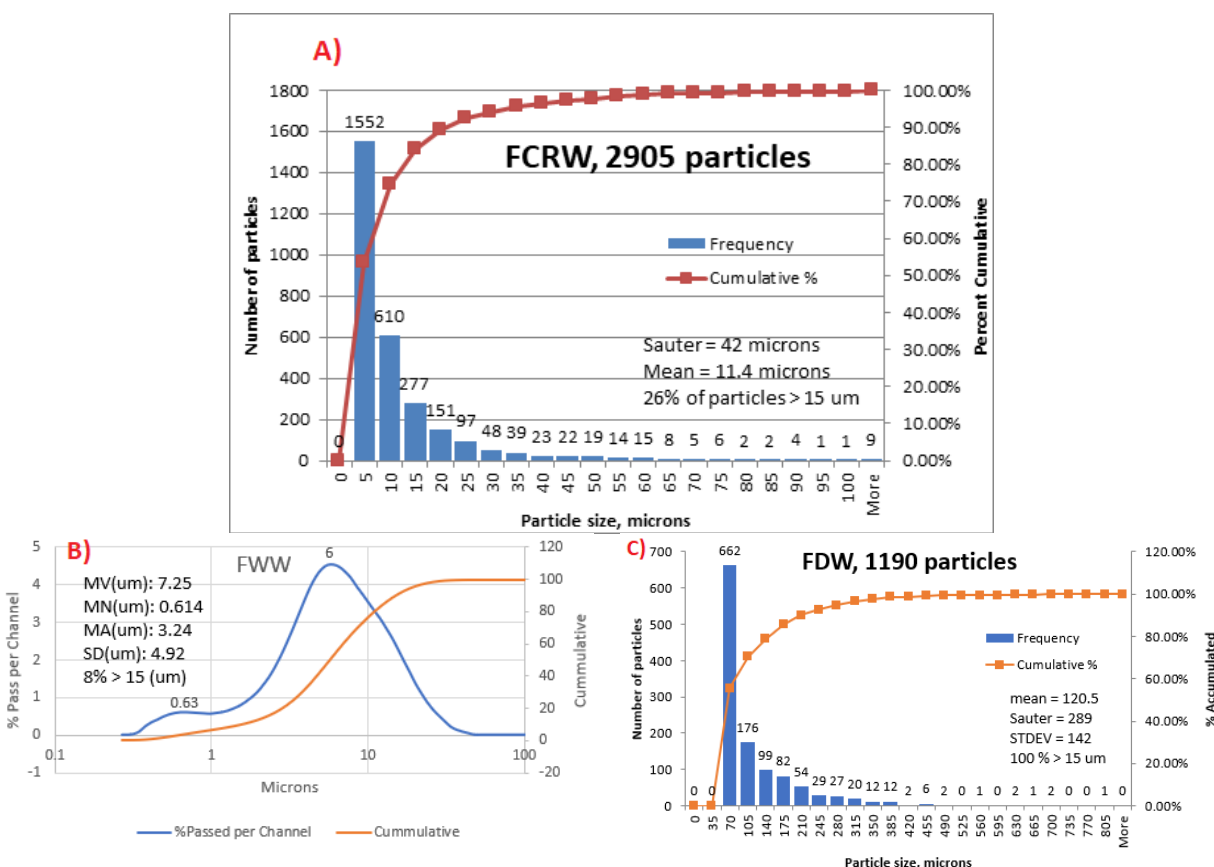


Figure 7. Particle size distribution of A) FCRW, B) FWW, and C) FDW. Note: Microtrac results are shown for the FWW sample. Histogram of photos are shown for the FCRW and FDW samples.

The FCRW solids had a mean diameter of 11.4 microns and approximately 26% of the particles had a diameter larger than 15 microns. 15 microns is an estimated particle dimension limit above which impact damage (erosion) is expected and it is thought to cause damage to the pump seals. The impact energy of large particles can damage the pump seals. This might be a significant concentration of solids that can act as an abrasive on the pump seal faces. The FWW solids samples had a smaller average diameter (7.2 microns) and 8% of the particles had a diameter larger than 15 microns. The smaller diameter observed in the Microtrac results shows the better size discrimination with the laser scattering. All solids in the FDW samples were larger than 15 microns. Please note that when analyzing an optical picture of particles, the

smallest particles tend to be left out during the segmentation of the image (separating particles from background) and the results are more concentrated on larger particles. In the case of the FDW solids samples, given their large diameters, a filter (for example 0.45 microns) can easily remove particles from solution.

3.1.3 Summary of the FCRW, FDW, and FWW samples

The large amount of settled solids found in the FCRW sample was mostly iron oxide (magnetite) and silica (Quartz). A significant percent of these solids (23%) had diameters larger than 15 microns with irregular shape. Similarly, a significant number of solids were found in the FWW sample. They were mostly iron oxide (magnetite) and only 8% of the particles were larger than 15 microns. A lesser number of solids, mostly kaolin, were found in the FDW sample but all particles were bigger than 15 microns. Recall, pump seals of the type used at 241-17F and 241-49H are sensitive to a few ppm of insoluble solids.

3.1.4 Analysis of the HCRW, HDW, and HWW samples

Compound (XRD and FTIR) and Elemental Analysis (XRF, SEM/EDS, and ICP-OES)

The crystalline minerals identified in the XRD spectra of the HCRW, as shown in Figure 8, included lepidocrocite (FeOOH), goethite (FeOOH), and magnetite (Fe_3O_4) along with a large background shift possibly due to the amorphous polymeric filter. The presence of oxyhydroxide and oxide is an indication of aging (thermal) experienced by the iron (possibly Fe^{2+}) in the HCRW sample. Possibly, soluble iron from either a source water or corrosion at the pump units experienced some higher temperature, possibly from the pump units, and hence changed the solubility limits. Some compounds may have precipitated and continued to age to a fully dehydrated compound like magnetite. No XRD signal was observed in the HDW and HWW samples.

The compound identified in the FTIR spectrum of the HCRW samples, as shown in Figure 9, included iron oxide and chromate oxide (CrO_4^{2-}). Again, chromium is being co-precipitated. There may be some aluminosilicate, but the signal was too weak. The chromate was not observed in the XRD spectrum. Therefore, it must be amorphous. The ICP-OES of the digested solids did confirm the presence of chromate. This case is like the case of the FCRW sample where chromates were observed, and it may suggest a precipitation reaction of the chromate. In the case of the HDW solid samples, aluminosilicate, magnetite, carbonate, nitrate and possible borates were observed. Gibbsite, kaolin, and some organic were observed in the FTIR analysis of the HWW samples. A few common solids such as iron oxide was found in HWW, HDW, and HCRW solids.

An EDS spectrum of the HCRW samples identified Fe, Cr, Al, Si, Zn, and Cu (see Figure 10). The presence transition metals can't confirm if the metals sources are from metal corrosion or direct transfer from source water (DW & WW). Both the HDW and HWW contain Fe, Al, and Si. Phosphorous (P) was also observed. Figure 10 also show that sample HDW is a solid cake and only a few particles are observed in the HCRW sample. A significant number of solids was observed in the HWW sample.

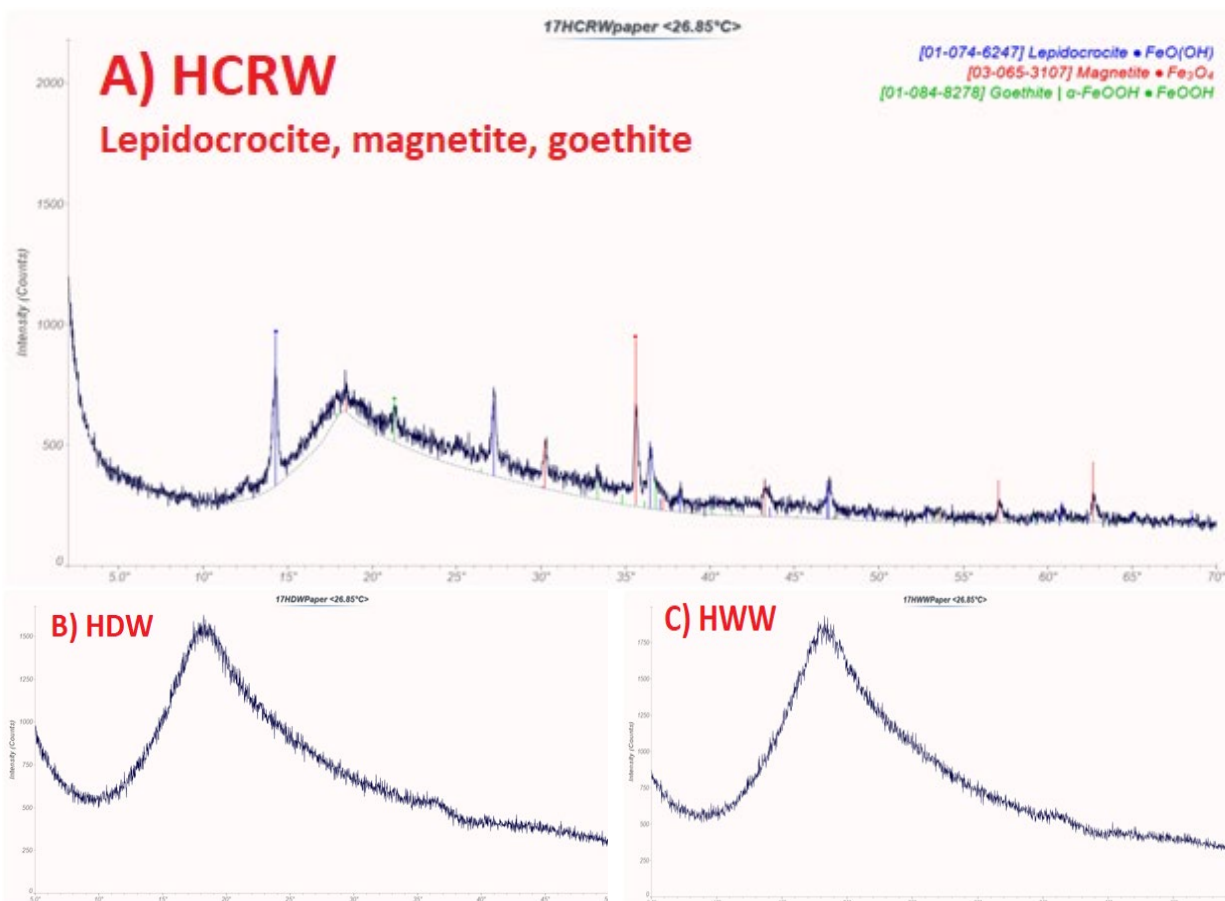


Figure 8. XRD spectra of the HCRW, HDW, and HWW solid samples.

More elements were observed in the XRF spectra of the H-area water samples. Figure 11 shows the XRF spectra of the HCRW, HDW, and HWW solid samples. In the HCRW sample, Fe, Zn, Cr, Ca, Ba, Si, and Cu were observed (Figure 11A). The Ca, Ba, Zn, and Cu are probably from the source water (HDW and/or HWW). As noted, before, iron can come from the source water and/or corrosion reactions. Both the HDW and HWW solid samples had Fe, Al, Ca, Ni, Cu, and Mn. Some of these elements like Al and Mn are not present in the HCRW sample indicating that HCRW is a network of Fe, Cr, Si oxides and a charge balancer like Ca or Ba. Yttrium is only found in groundwater as only seen in the XRF spectrum of the HWW sample.

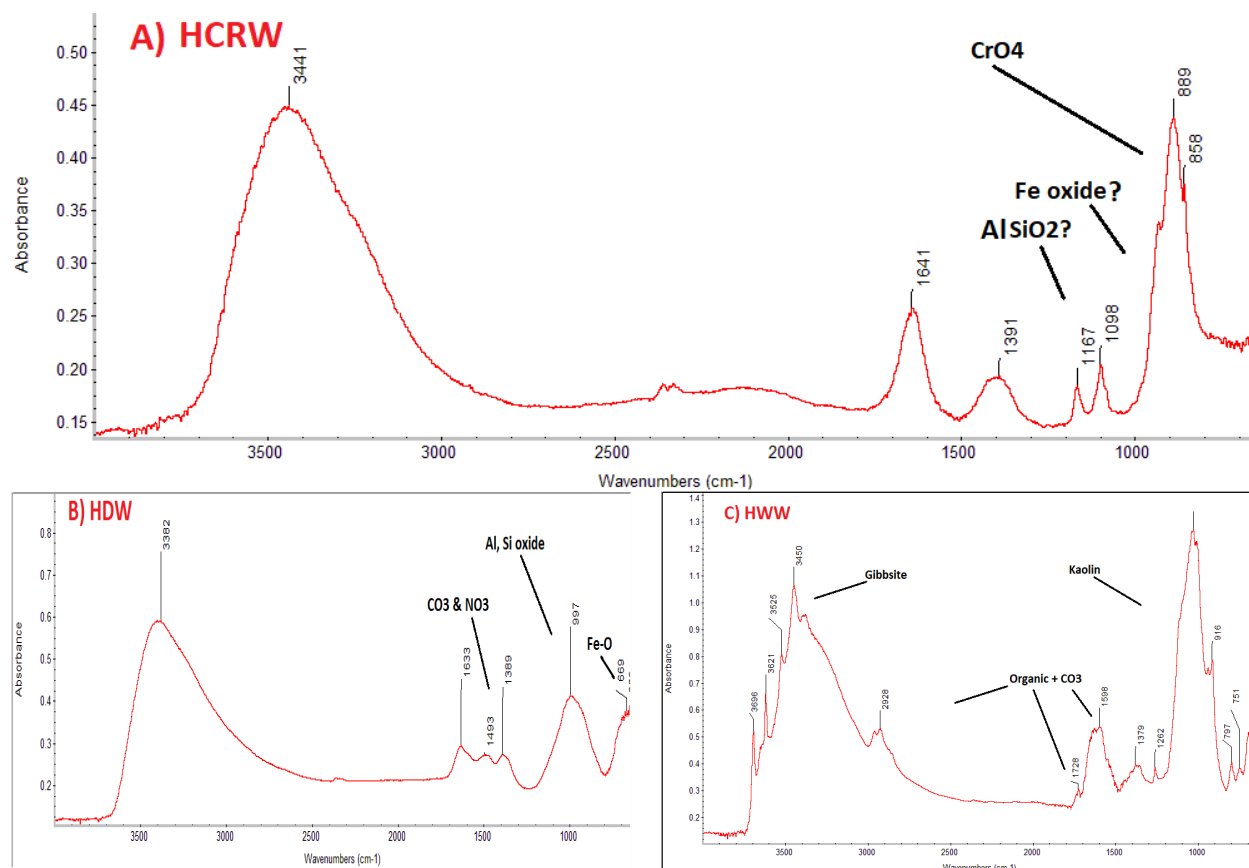


Figure 9. FTIR of the HCRW, HDW, and HWW solids.

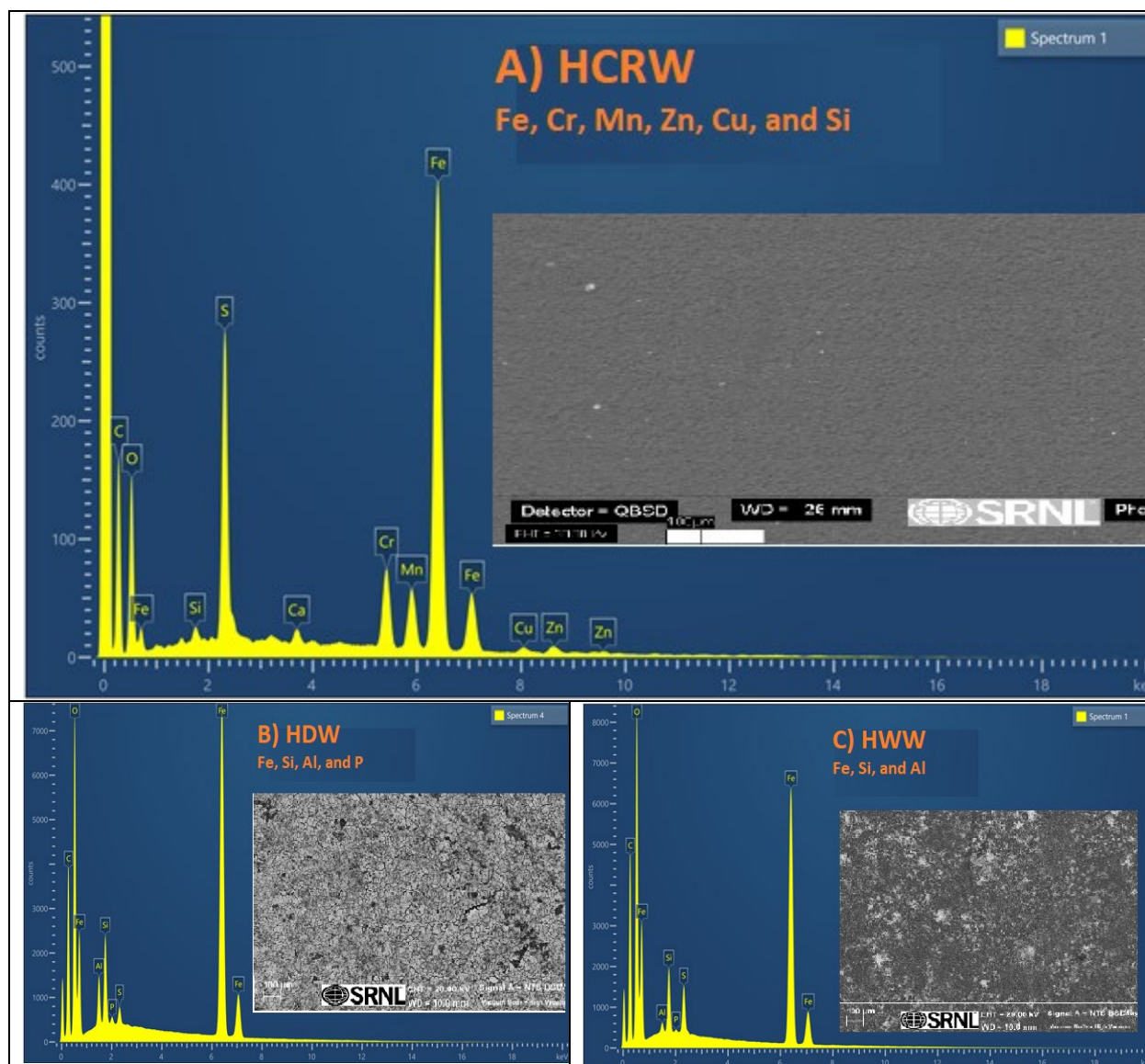


Figure 10. SEM/EDS analysis of the A) HCRW, B) HDW, and C) HWW samples

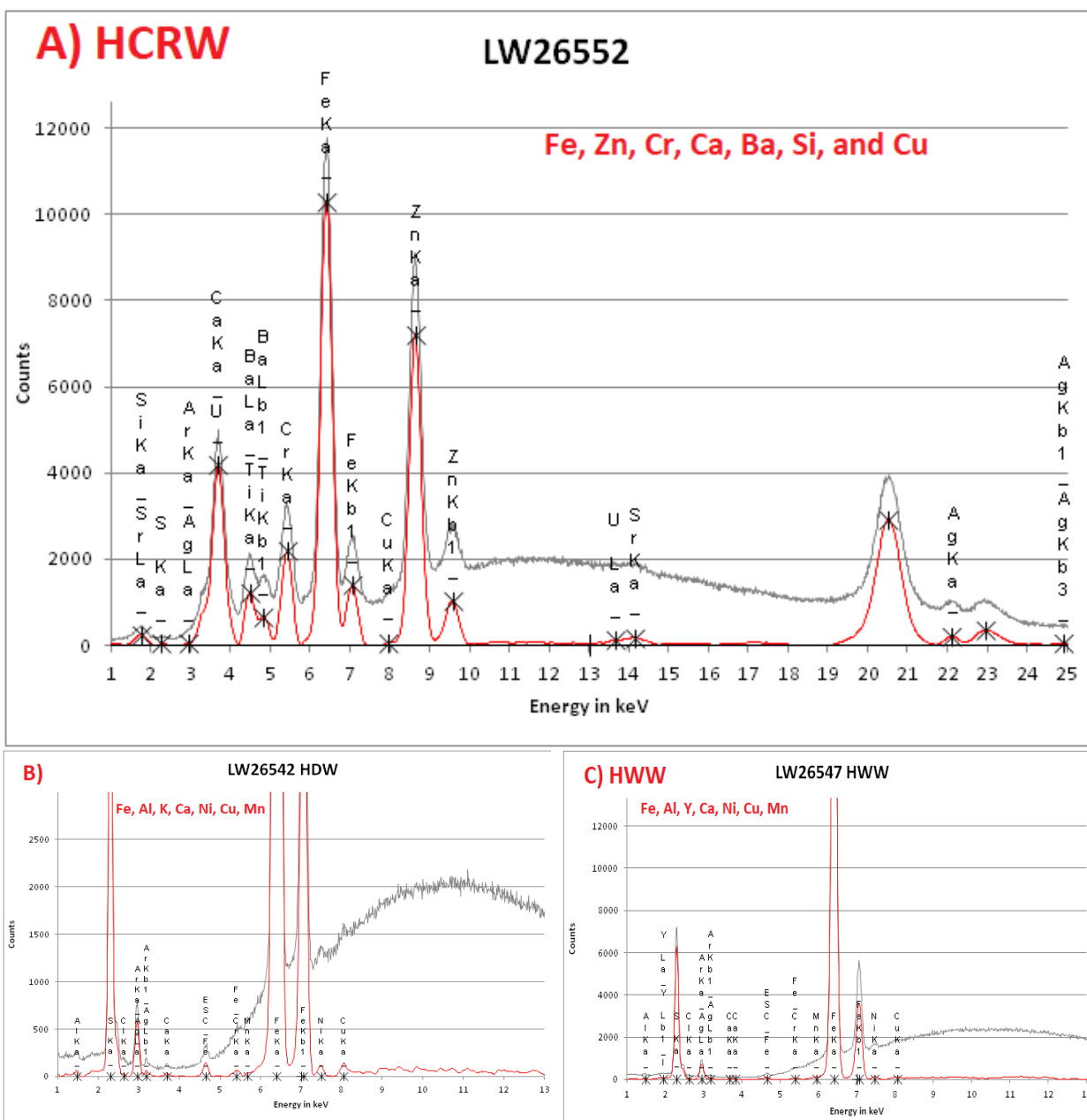


Figure 11. XRF elemental composition of A) HCRW, B) HDW, and C) HWW.

The ICP-OES results of the digested HCRW, HDW, and HWW samples are presented in Table 3. The predominant elemental components of the HCRW liquid sample were Al, B, Ba, Ca, Cr (~280 ug/g_{slurry}), Fe, Mg, Na, S, Si, and Zn. The less than expected concentration of elemental chromium is consistent with the EDS, XRF, and FTIR results that indicated part of the added chromium precipitated and formed part of the solids. Silicon concentration is much lower in the HCRW sample compared to the HDW and HWW samples possibly due to precipitation. Overall, both HWW and HDW have similar elemental concentrations. Table 3 also shows the digestion of the solids from HCRW, and the major elements were Al, Fe, Cr, and Zn consistent with the other analysis.

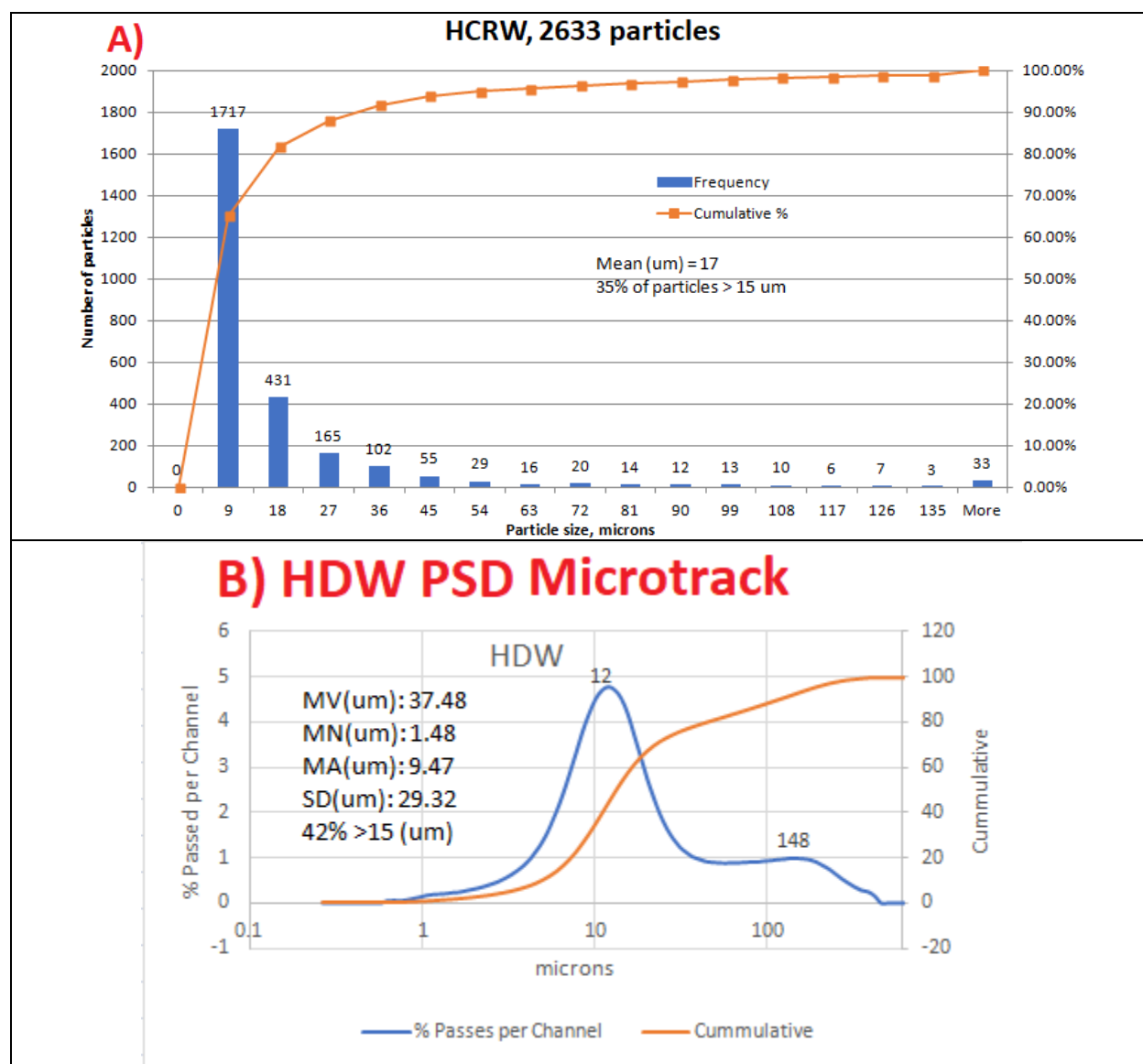
Table 2. ICP-OES analysis of the slurry samples from HCRW, HDW, HWW slurries (ug/g_{slurry}) and solids from HCRW (mg)

Element	HDW	HWW	HCRW	HCRW Solids (mg)#
Ag	< 0.18	< 0.18	< 0.17	< 0.054
Al	0.165	< 0.1	0.145	0.066
B	1.04	0.853	0.245	< 0.003
Ba	0.259	< 0.03	0.112	< 0.009
Be	< 0	< 0	< 0	< 0.001
Ca	2.51	2.10	0.306	0.4145
Cd	< 0	< 0	< 0	< 0.001
Ce	< 0.07	< 0.07	< 0.07	< 0.074
Co	< 0.02	< 0.02	< 0.02	< 0.002
Cr	< 0.04	< 0.04	280	0.1525
Cu	< 0.06	< 0.07	< 0.06	< 0.017
Fe	5.19	3.52	1.70	0.4725
Gd	< 0.09	< 0.1	< 0.09	< 0.0019
K	< 0.83	< 0.84	< 0.81	< 0.198
La	< 0	< 0	< 0	< 0.001
Li	< 0.10	< 0.06	< 0.06	< 0.018
Mg	0.385	0.424	0.051	0.0497
Mn	0.062	0.108	< 0.02	< 0.006
Mo	< 0.03	< 0.03	< 0.03	< 0.004
Na	3.32	2.89	377	NR
Ni	< 0.02	< 0.02	< 0.02	< 0.002
P	< 0.07	< 0.07	< 0.07	< 0.016
Pb	< 0.06	< 0.06	< 0.06	< 0.019
S	3.27	3.09	12.2	1.68
Sb	< 0.04	< 0.04	< 0.0	< 0.01
Si	5.72	5.25	1.85	< 0.121
Sn	< 0.2	< 0.2	< 0.2	< 0.062
Sr	< 0.01	< 0.01	< 0.01	< 0.002
Th	< 0.00	< 0.1	< 0.1	< 0.01
Ti	< 0.0	< 0.04	< 0.04	< 0.007
U	< 0.24	< 0.25	< 0.24	< 0.026
V	< 0.03	< 0.03	< 0.03	< 0.01
Zn	< 0.05	< 0.05	0.267	0.0466
Zr	< 0.01	< 0.01	< 0.01	NR

NR stands for "not reported". #Digested solids.

3.1.5 Particle size distribution of the HCRW, HDW, and HWW

As stated earlier, two approaches were used to determine the particle size distribution. Microtrac results were obtained only from the HDW sample (see Figure 12B). Due to their low solid concentrations, optical image analysis was performed on the images of the HCRW and HWW samples (see Figure 12A and 12C). The mean particle size of the HCRW sample was 17 microns and 35% of the particles had a diameter larger than 15 microns (see Figure 12A). Such a high fraction of particles can potentially plug narrow conduits. The mean particle diameter of the HDW solids was 37.5 microns and 42% of the particles had a diameter larger than 15 microns. Finally, the mean particle diameter of the HWW particles was 9.3 microns and 23% of the particle had a 15 microns diameter or larger.



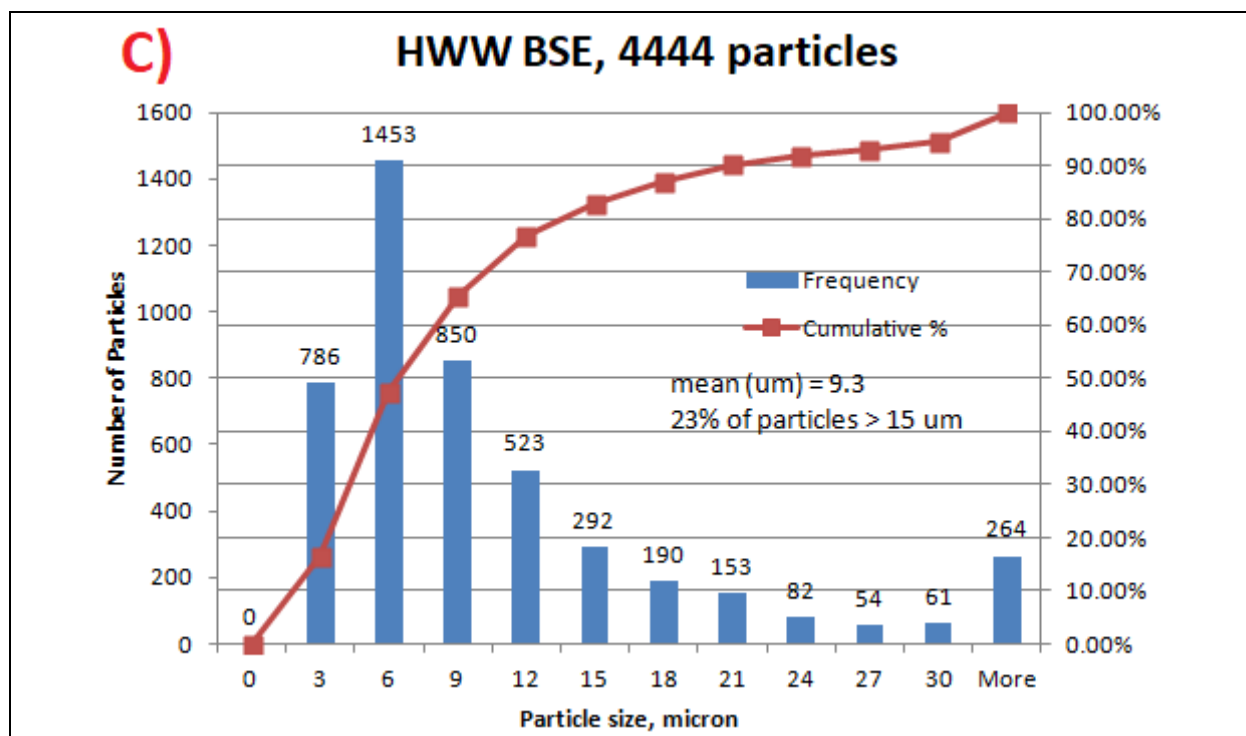


Figure 12. Particle size analysis of the HCRW, HDW, and HWW samples.

3.1.6 Summary information of the HCRW, HWW, HDW, FCRW, FDW, and FWW.

A summary of the findings in this work is listed in Table 4. As shown in the table, iron and silicon were the most common elements in the solids. The size and quantity of solids found were not, in some case, negligible. The gravimetric data indicates that the HCRW samples had more insoluble and soluble solids than the FCRW, and it is expected that HCRW sample to cause more problems to the pump seals. Iron, zinc, aluminum, silicon and chromium form precipitates at pH higher than 8. The soluble solid levels measured are sufficient to form solids if the cooling liquid is exposed to a pH or temperature shock as well as any evaporation. It is recommended that filtration after pH adjustment is made and to minimize the soluble solid content of the pump cooling water

Table 4. Summary Information of the HCRW, HDW, HWW, FCRW, FDW, and FWW

Analyses	HCRW	HDW	HWW	FCRW	FDW	FWW
Liquid Density (g/mL at 22.7 °C)	0.9984	0.994	0.995	0.9985	0.994	0.996
pH	9	6	6	9	6	6
Gravimetry (Solids) (mg/L)	Insoluble 5.9 Soluble 1320	Insoluble 2.3 Soluble 28	Insoluble < 1 Soluble 102	Insoluble 1.7 Soluble 1265	Insoluble <1 Soluble 84	Insoluble 9.4 Soluble 28
XRD mineralogy	Lepidocrocite, goethite, and magnetite	Below detection limit	Below detection limit	Magnetite, SiO ₂ , Quartz	Below detection	Lepidocrocite Magnetite
SEM/EDS elemental	Fe, Cr, Al, Si, Zn, and Cu	Fe, Si, Al, and P	Fe, Si, and Al	Al, Si, Cr, Fe, and Zn	Al, Si, Fe, Ca, Cu, Cl, K, and Mg	Fe, Si, and Al
XRF Elemental composition	Fe, Zn, Cr, Ca, Ba, Si, and Cu	Fe, Al, K, Ca, Ni, Cu, and Mn	Fe, Al, Y, Ca, Ni, Cu, and Mn	Zn, Fe, Ca, K, Cu	Fe, Ni, Cu, K, Y, Cl, and Ca	Fe, Zn, Cu, Ni, Cr, Ca, Al, Cl, and Mn
FT-IR	Chromate, iron oxide, SiO ₂	Aluminosilicate, iron oxide, carbonates and nitrates	Kaolin, Gibbsite, carbonate, organic	Chromate, iron oxide, SiO ₂	Kaolin and carboxylates	Lepidocrocite, nitrates, & borates
ICP-OES*	Al, B, Ba, Ca, Fe, Mg, Na, S, Si, and Zn	Al, B, Ba, Ca, Fe, Mg, Mn, Na, S, and Si	B, Ca, Fe, Mg, Mn, Na, S, and Si	B, Ba, Ca, Cr, Fe, Mg, Na, S, Si, and Zn	B, Ba, Ca, Fe, Mg, Na, S, and Si	B, Ba, Ca, Fe, Mg, Mn, Na, S, and Si
Particle Size Analysis (PSA)	0 – 155 µm Mean at 17 µm SD = 26 µm 35% greater than 15 µm	0.9 – 180 µm Mean at 37.5 µm SD =29 µm 42% greater than 15 µm	3 – 45 µm Mean at 9.3 µm SD = 16 µm 23% greater than 15 µm	5 -150 µm Mean(µm) at 11.4 SD = 21 µm 26% greater than 15 µm	0.4 – 39 µm Mean at 120 µm SD = 142 µm 100% greater than 15 µm	70 – 869 µm Mean at 7.2 µm SD = 4.9 µm 8% greater than 15 µm

* Elements with concentration above the detection limit in the ICP-OAES. The relative standard error is 10% at the 2-sigma confidence interval.

4.0 Conclusions

Six different water samples from 241-17F and 241-49H were analyzed for chemical analysis and determinations made for the physical characteristics of any insoluble solids in these samples. The insoluble solids found in the FCRW (F-Area caustic water treated with sodium chromate at 241-17F) sample are mostly magnetite (Fe_3O_4 or possibly rust which is a mixture of hematite, iron oxide hydroxide and iron hydroxide) and silica. 26% of FCRW particles have at least one dimension larger than 15 microns. The insoluble particles of the source water, domestic water (FDW), are mostly kaolin (aluminosilicate) and some iron oxide. All particles were larger than 15 microns. The insoluble particles of the other source water, well water (FWW), were mostly iron oxide with some trapped cations like calcium. Only 8% of FFW particles were bigger than 15 microns.

The insoluble particles found in the H-area chromate water (caustic water treated with sodium chromate) are mostly iron oxide, chromate, and silica. Approximately 35% of H-area chromate water particles were larger than 15 microns and they had irregular shape. The settled particles found in the domestic source water (HDW) were mostly silicates and iron oxide. At least 42% of HDW particles had one dimension larger than 15 microns. The other source of water in H-area, well water (HWW), had a noticeable amount of kaolin and gibbsite insoluble particles. Nearly 23% of HWW particles had at least one dimension larger than 15 microns.

The large particles (greater than 15 microns) may have cause kinetic impact damage to the pump seal. The damage may have caused debris (particles of various sizes). In addition, particles from the source water (well water and domestic water) may have come from the soil or formed from corrosion with commercial pipes were part of the chromate water and these particles may enter narrow conduits and act like abrasives scratching or deforming or interrupting movement of surfaces such as in a sealed pump. The particles appear to form either during the making of the chromate water or during service from possible oxidation and/or reduction reactions with the chemicals and materials encountered by the chromate water. Particle formation and growth may also be occurring as a result of thermal aging, during pumping operation as a potential heat source (some seals at 241-17F and 241-49H did not have proper venting allowing some heat buildup). This is most clearly seen in the HCRW sample where different stages of particle growth were detected ($\text{Fe}^{2+} \Rightarrow \text{Fe}(\text{OH})_x^{3-x} \Rightarrow \text{FeOOH}$ and $\text{Fe}(\text{OH})_x^{3-x} \Rightarrow \text{Fe}_3\text{O}_4$ at $\text{pH} > 8$). Please note the new FTF pumps did not have seal flush lines which allow air removal from the seal compartments. A mechanical postmortem of damaged seals revealed signs of overheating (see Appendix D). The lack of venting most likely allowed the seals to run dry and experience high temperature damage in addition to any particles on the carbon/silicon carbide face materials. If liquid gets between the pump seal interface, it will dry and deposit particles that can in turn damage pump seal faces. The zinc was observed in both chromate water (F and A-area) and it is a clear indication of corrosion of galvanized steel (for example, galvanic coupling with a more noble metal like copper or aluminum). This only happened after the source water (domestic or well) was chromate treated (although zinc was observed in the well water from F-area to begin with) in both A and F-area. The expected reaction $\text{Zn}^{2+} \Rightarrow \text{ZnO}_2^{2-} \Rightarrow \text{Zn}(\text{OH})_2$ contributed to the solid's accumulation. Finally, chromium is being co-precipitated to form a hard solid chromium chromate during chromate addition to the caustic water (corrosion from stainless steel is unlikely). The H-area chromate water had the most solids (the H-area domestic water brought aluminum over) with the highest number of particles larger than 15 microns. Therefore, the H-area chromate water should impart the most frequent pump seal damages. The soluble solid concentration is double that of the recommended concentration (400 ppm from Ref. 2) for these seals. All seals leak small amount of product liquid and at these soluble solid concentrations, particles will form on the air size of the sealing faces interface possibly causing tear.

The chromate was also coprecipitated with the iron and zinc as an indication of fast precipitation. It is recommended that a combination of filtration, if it is not being done currently, and iron reduction is needed. A potential source of the iron can come from severe metal corrosion such as galvanic coupling between a galvanized mild steel and other metals like aluminum or copper. Chemicals addition to poison a corrosion

reaction could be explored further. As mentioned earlier it is recommended to keep the soluble and insoluble content of the cooling water to just a few ppm at most to lower the risk of solid precipitation in the event of a pH shock (pH raised to 9 or higher), a temperature shock (loss of ventilation or running dried) or an evaporation that the cooling liquid may experience. Sources of soluble solids like transition metals, silica, and aluminum from the source water (well water and domestic water) and any metal corrosion (galvanic coupling to a galvanized steel) should be avoided or maintained to a minimum.

Appendix A: SRNL Scope for the Characterization of the soluble and insoluble portions of the FCRW, FDW, FWW, HCRW, HDW, and HWW water samples

SRNL Scope

1. Characterize the soluble and insoluble portions of solids from 241-17F and 241-49H domestic water, well water, and chromate water from each facility respectively.
 - a. Filtered solids
 - i. SEM-EDS – Size and elemental composition
 - ii. XRD – Crystalline/semi-crystalline structure
 - iii. XRF-Elemental composition
 - iv. FTIR – Structural/Molecular composition and organic detection
 - v. Microtrac – Slurry is suspended for laser light scattering analyses
 - vi. Photography analysis if Microtrac data is not obtained
 - b. Filtered solids digestion
 - i. Digest solids with peroxide fusion (PF) for RCRA metals.
 - ii. ICP-OES or ICP-AES for elemental composition of leachate
 - c. Slurry digestion
 - i. Digest solids or slurry with aqua-regia (AR). Digest solids with peroxide fusion (PF) for metals.
 - ii. ICP-OES or ICP-AES for elemental composition of leachate

Appendix B. Examples of particle size distribution of different images from different sources (SEM, optical photography, and optical microscopy).

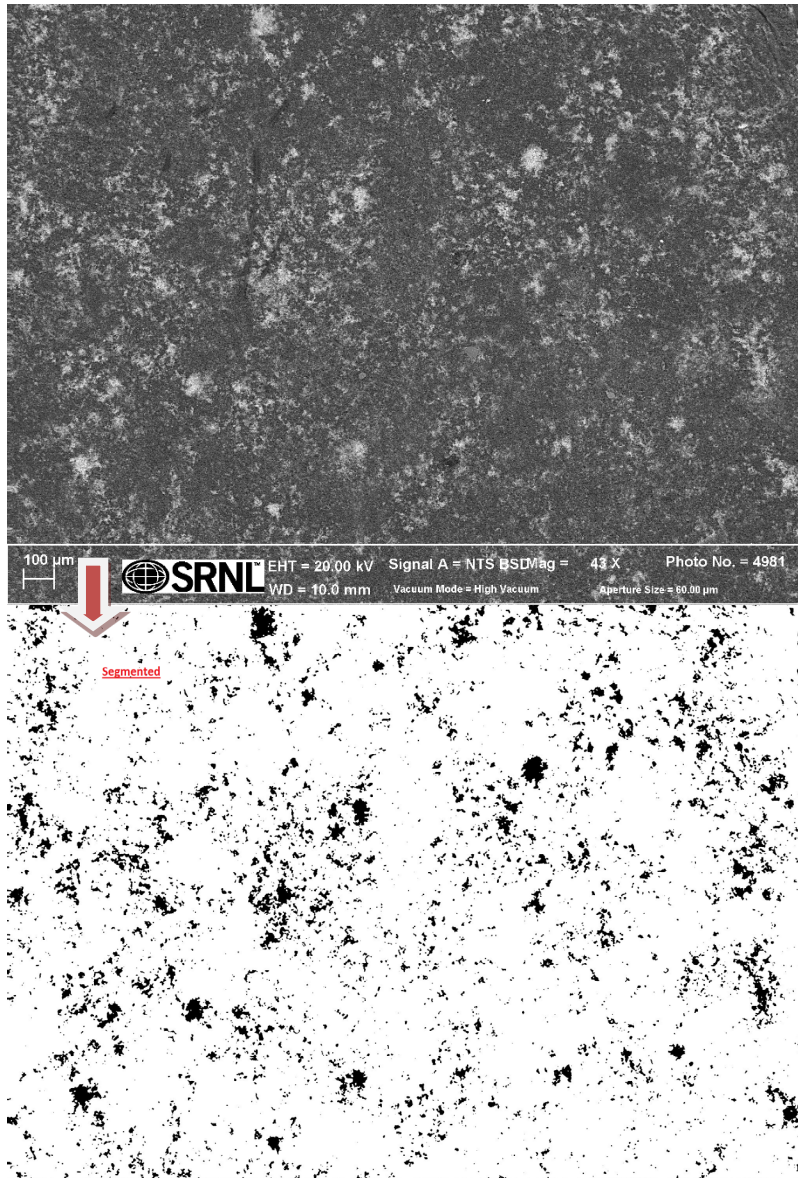


Figure 13. An example of a black and white image segmentation done with an SEM image of the HWW solids. Segmented image does not include captions of the original image (top)

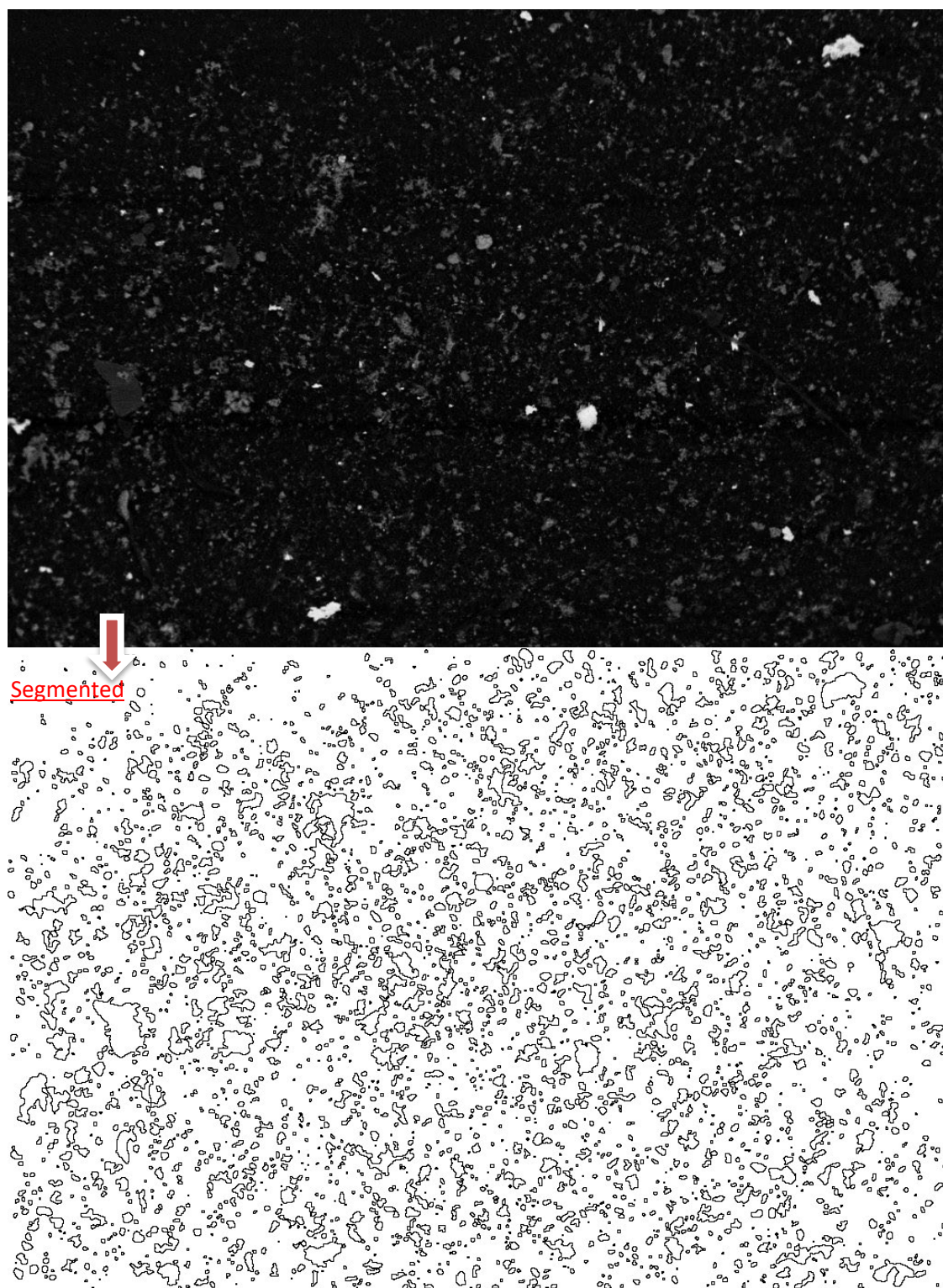


Figure 14 An example of a black and white image segmentation done with an BE image of the FCRW solids.
Segmented image does not include captions of the original image (top)

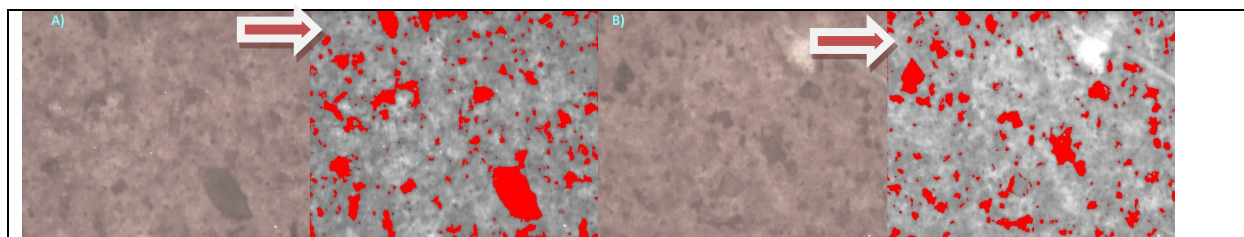


Figure 15. An example of image segmentation (images with red particles) of the optical microscope images of FDW solids.

Appendix C. Analytical Methods

FT-IR spectroscopy is the application of modulated infrared light to a sample to excite its vibrational modes. The vibrational modes are unique for each sample and it can be used to identify chemical substances or functional groups (organic and inorganic materials) in solid, liquid, or gaseous forms. FT-IR spectroscopy is also used to characterize new materials or identify and verify known and unknown samples.

Inductively coupled plasma atomic emission spectroscopy (ICP-AES) is an emission spectroscopy that identifies and quantifies the elemental composition of samples. ICP-AES is based on exciting the metal atoms/ions of the samples by forming a plasma and analyzing the emission wavelength of the electromagnetic radiation, which is typical of that metal or element of interest.

X-ray diffraction analysis (XRD) is a technique used in materials science to determine and identify the crystallographic structure of a material or mineral. XRD works by irradiating a material with incident X-rays and then measuring the intensities and scattering angles of the X-rays that leave the material.

X-ray fluorescence analysis (XRF) is a technique used in materials science to determine and identify the elemental composition of a material or mineral. XRF works by irradiating a material with incident X-rays and then measuring the intensities of the X-rays that leave the material. Some of the X-rays contain unique information on the electron binding energies inside the sample atoms.

Energy dispersive X-ray spectroscopy (EDS) is an analytical method for chemical characterization of materials. The sample is bombarded with a beam of electrons to excite the sample. The sample relaxes by emitting X-rays some of which are characteristics of the electron binding energy in the sample's atoms. EDS systems are generally attached to an electron microscopy instrument such as transmission electron microscopy (TEM) or **scanning electron microscopy (SEM)**.

Particle size analysis (PSA) is laboratory techniques which determines the size range, and/or the average, or mean size of the particles in a powder or liquid sample. Microtrac utilizes a set of lasers that impinges on the suspended slurry sample, and the scattered light is measured at differently position detectors. The data and its processing generate a particle size distribution of the sample. Optical microscopy photos are used for deriving a particles size distribution whenever the solid concentration of the sample is below the minimum solid concentration for the Microtrac analysis which is typically 0.01% v/v.

Appendix D. Personal communication with Eric Burgin



Eric Burgin

Originally our new FTF pumps did not have seal flush lines which allow air removal from the seal compartments. The mechanical postmortem performed by John Crane Seal Co. indicated signs of overheating. The lack of venting most likely allowed the seals to run dry and experience high temperature damage in addition to any particles on the carbon/silicon carbide face materials. It sounds like some of the particles you found could be explained by these high temperatures.

DISTRIBUTION LIST:

Name	Electronic address
Azadeh Samadi-Dezfouli	Azadeh.Samadi-Dezfouli@srs.gov
Azikiwe Hooker	Azikiwe.Hooker@srs.gov
Eric Barrowclough	Eric.Barrowclough@srs.gov
Gregory Arthur	gregory.arthur@srs.gov
John Mccrary	John.Mccrary@srs.gov
John Occhipinti	john.occhipinti@srs.gov
John Tihey	john.tihey@srs.gov
John Windham	John.Windham@srs.gov
Mason Clark	Mason.Clark@srs.gov
Matthew Hoffman	Matthew.Hoffman@srs.gov
Phillip Norris	phillip.norris@srs.gov
Azikiwe Hooker	Azikiwe.Hooker@srs.gov
Jared Hughes	Jared.hughes@srs.gov
John Laukea	John.laukea@srs.gov
James Harris	James02.harris@srs.gov
Vijay Jain	vijay.jain@srs.gov
Boyd Wiedenman	boyd.wiedenman@srnl.doe.gov
Frank Pennebaker	frank.pennebaker@srnl.doe.gov
J. Eric Burgin	Eric.burgin@srs.gov
F. Fondeur	fernando.fondeur@srnl.doe.gov